

A Mini Course on the “Bigger Picture”

Before and After the Flow: Initial Conditions and High p_T jets

1. (strong) Quark Gluon Plasma: sQGP
2. Color Glass Condensate: CGC

M.Gyulassy and L. McLerran

Nucl.Phys.A750 (2005) 30

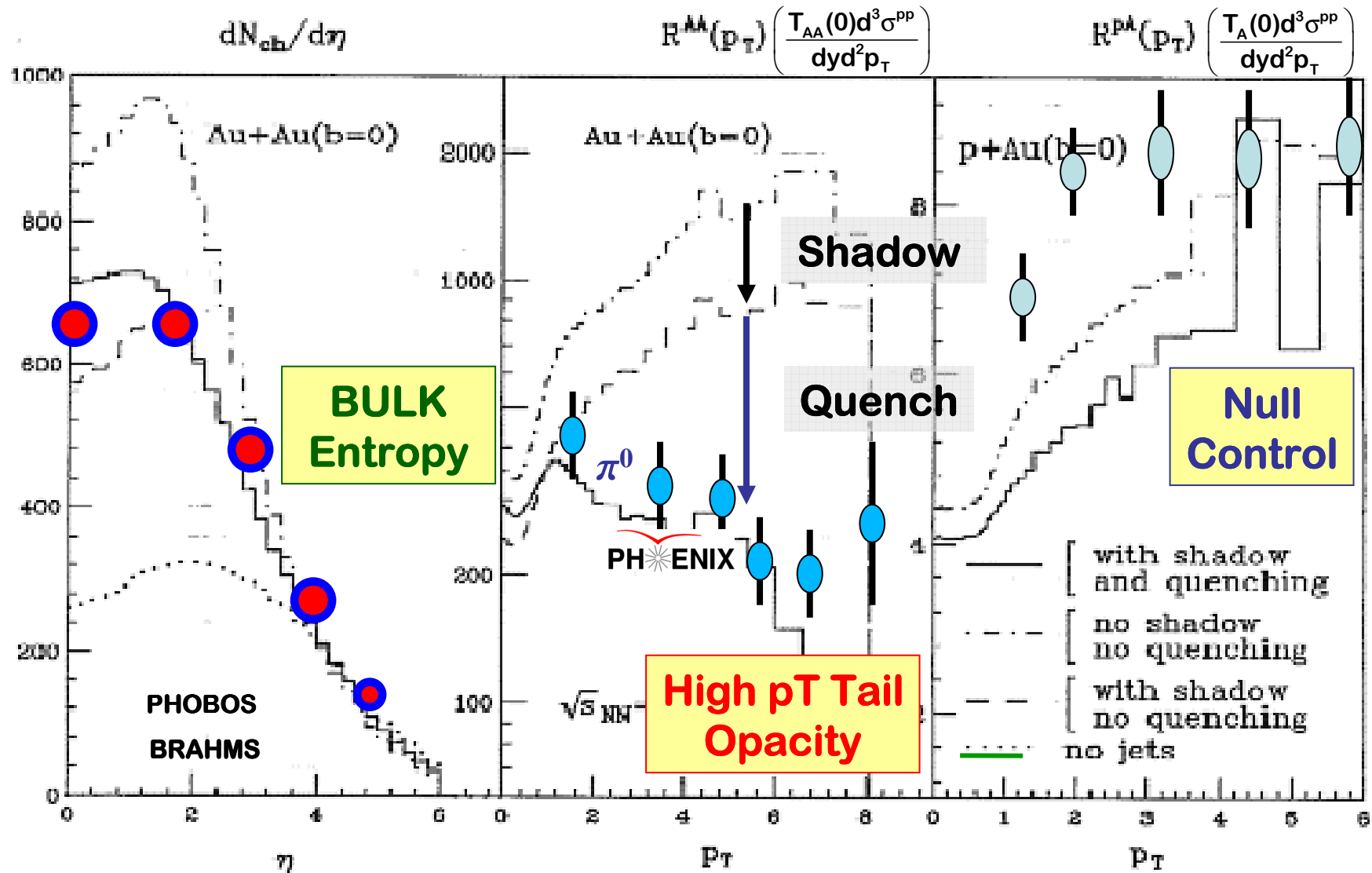
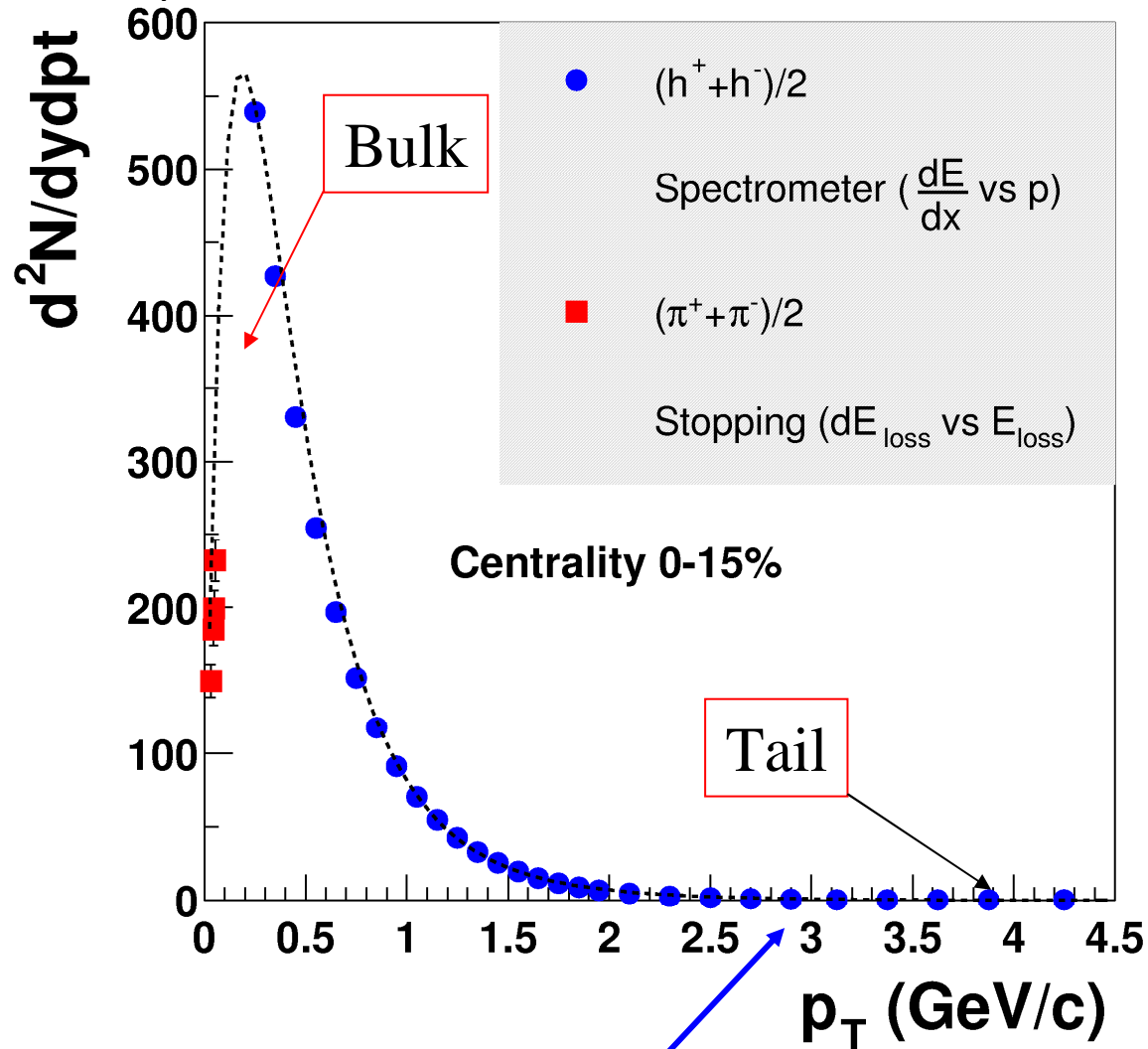


FIG. 1. Results of HIJING on the dependence of the inclusive charged-hadron spectra in central Au+Au and p+Au collisions on minijet production (dash-dotted line), gluon shadowing (dashed line), and jet quenching (solid line) assuming that gluon shadowing is identical to that of quarks and $dE/dl = 2$ GeV/fm with $\lambda_g = 1$ fm. $R^{AA}(p_T)$ is the ratio of the inclusive p_T spectrum of charged hadrons in A+B collisions to that of p+p.

p_T Distribution of Charged Particles



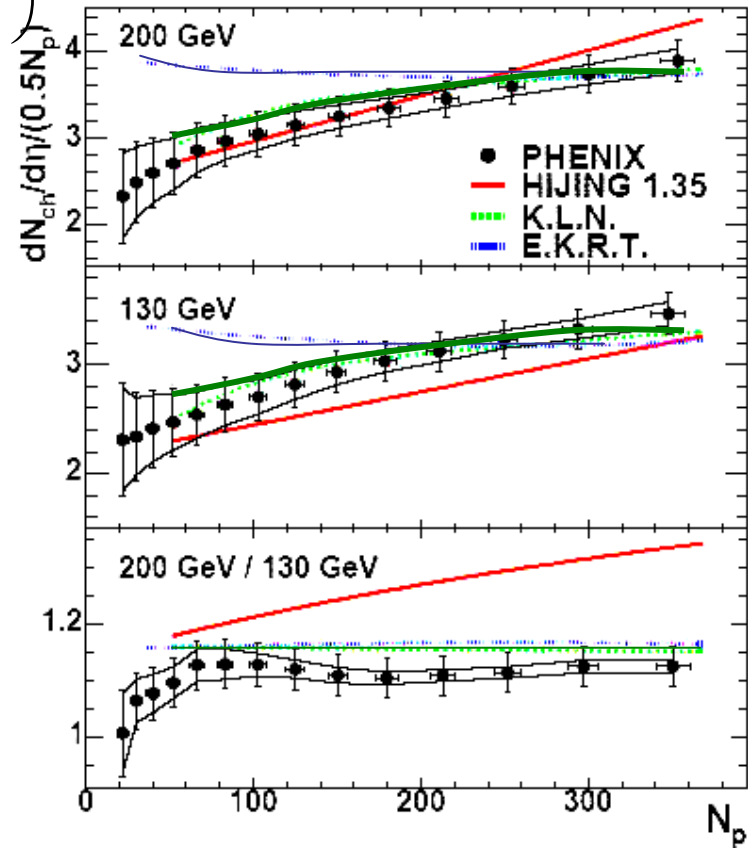
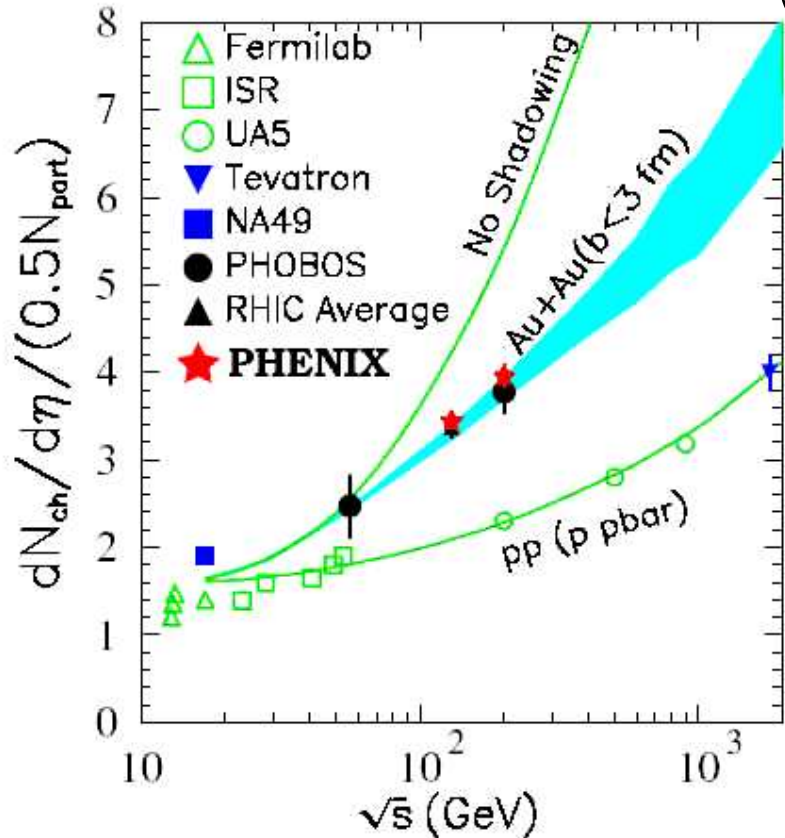
Phobos

G.Roland

We can use this tiny calibrated pQCD tail to probe the QGP Bulk!

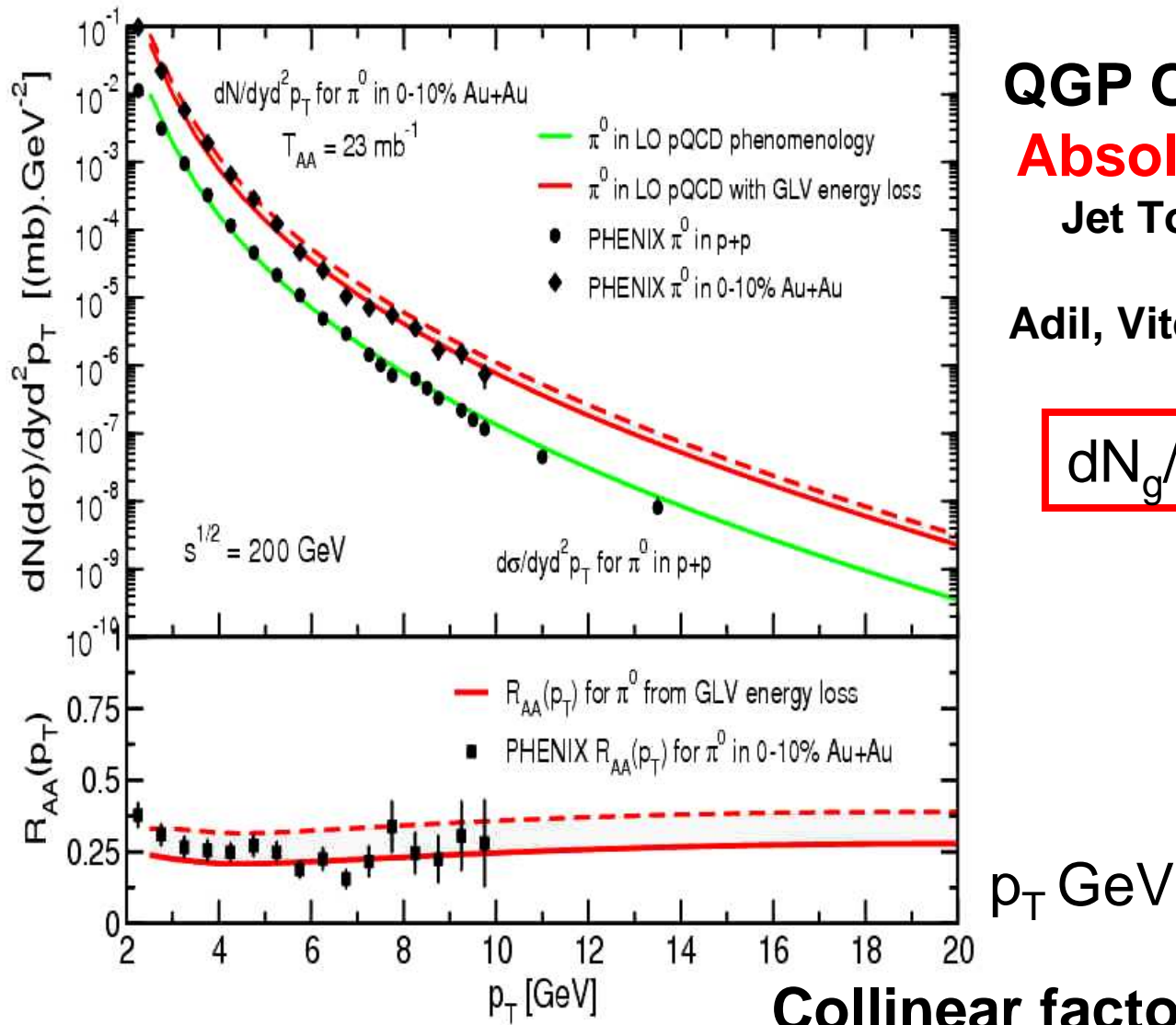
Evidence for saturating CGC initial conditions

$$Q_s^2(x, A) \approx 1 \text{ GeV}^2 \left(\frac{10^{-4}}{x} \right)^{0.3} A^{0.3}$$



$$N_{ch} = \rho_s N_{Part} + \rho_H(s) N_{BC}$$

Hard mini-jet ρ_H with **fixed** scale $Q_s = 2 \text{ GeV}$ fails.
 Q_s must vary with both s and N_{part}



QGP Opacity via Absolute Scale Jet Tomography

Adil, Vitev, MG (2005)

$$dN_g/dy=900-1200$$

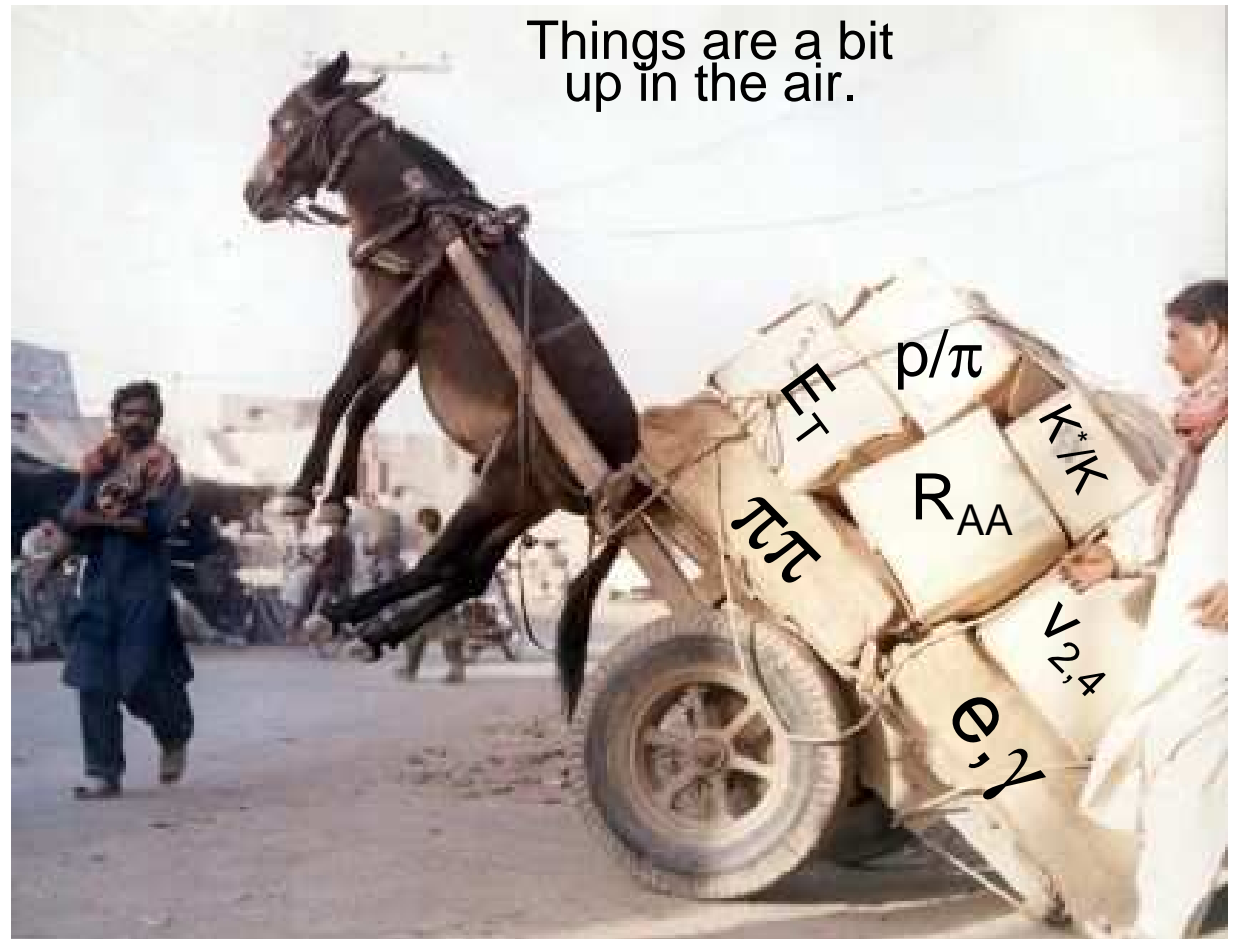
Collinear factorized pQCD

$$dN_{AB \rightarrow \pi} = T_{AB} \otimes \left(f_{a/A} \otimes f_{b/B} \right)_{\Delta k_T}^{\text{shad}} \otimes d\sigma_{ab \rightarrow c} \otimes P(\Delta E) \otimes D_{\pi/c}$$

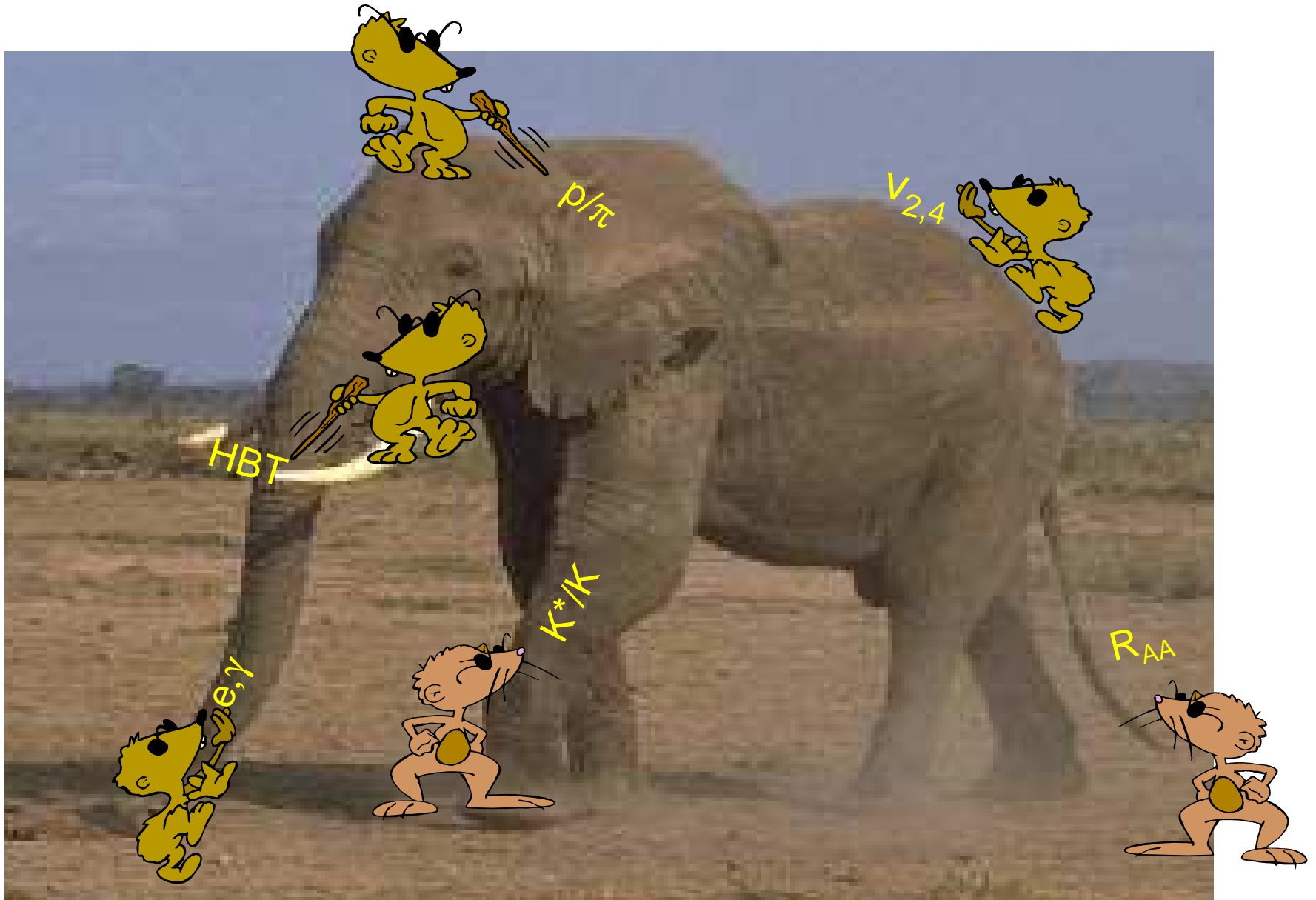
J.Cramers' Summary Slide of RHIC Physics in 2003

“The useful theoretical models that has served us so well at the AGS and SPS for heavy ion studies have now been overloaded with a large volume of puzzling new data from RHIC.”

“We need more theoretical help to meet the challenge of understanding what is going on in the RHIC regime.”



Experts have a hard time seeing the picture



Theoretical tools used at RHIC are built on rigorous **limits** of the Standard Model

1. Asymptotic free **perturbative pQCD**

Proton Spin structure (high $Q > 2 \text{ GeV}$)

Jets and heavy quarks (high $p_T > 10 \text{ GeV}$)

2. High temperature/density thermodynamics

nonperturbative **Lattice QCD**

Long Wavelength Collective (low $p_T < 1 \text{ GeV}$)

3. High energy **light cone QCD**

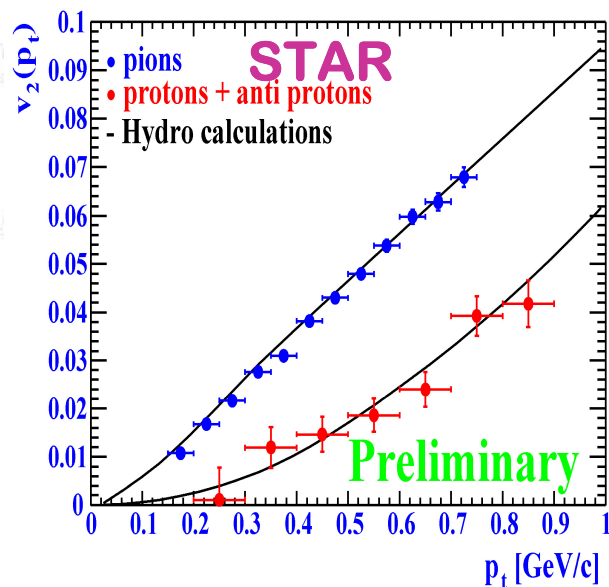
Color Glass Condensate (small $x < 0.001$)

“Day 1 New Physics” at RHIC

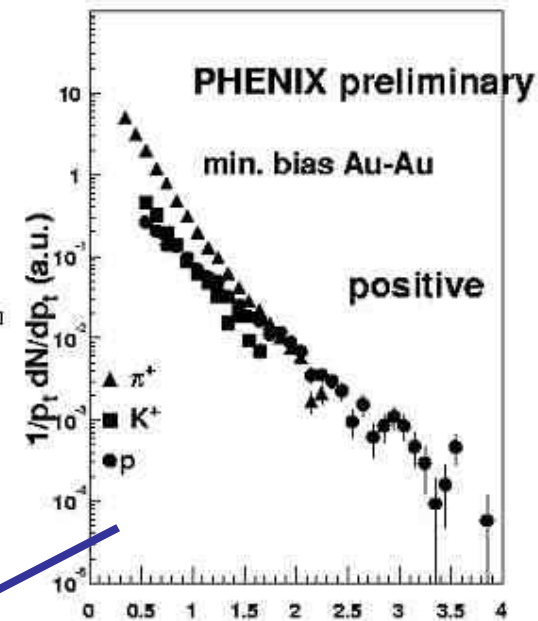
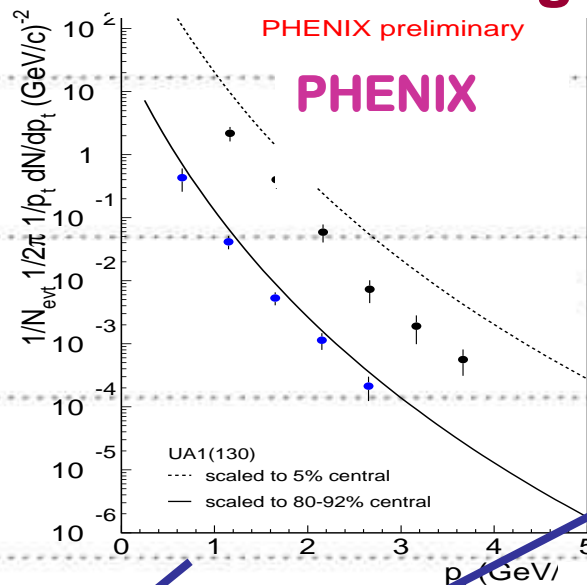
Baryon anomaly

1400

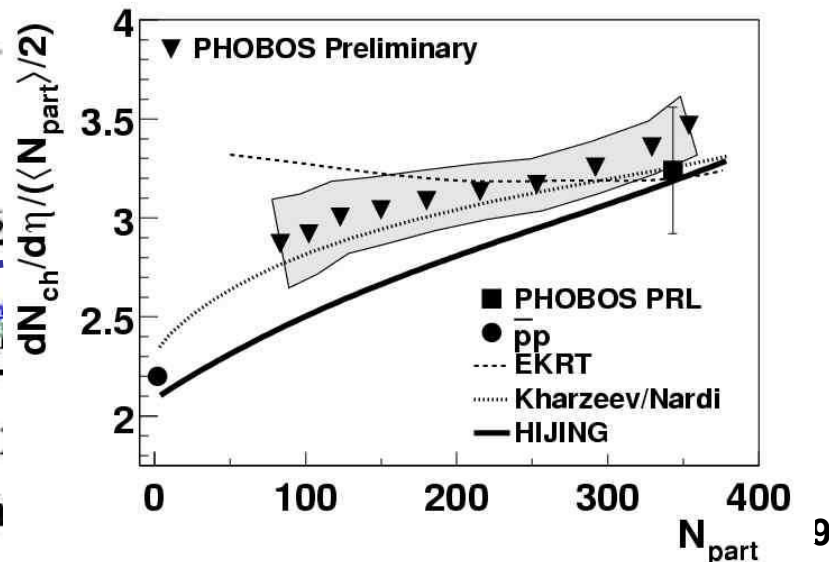
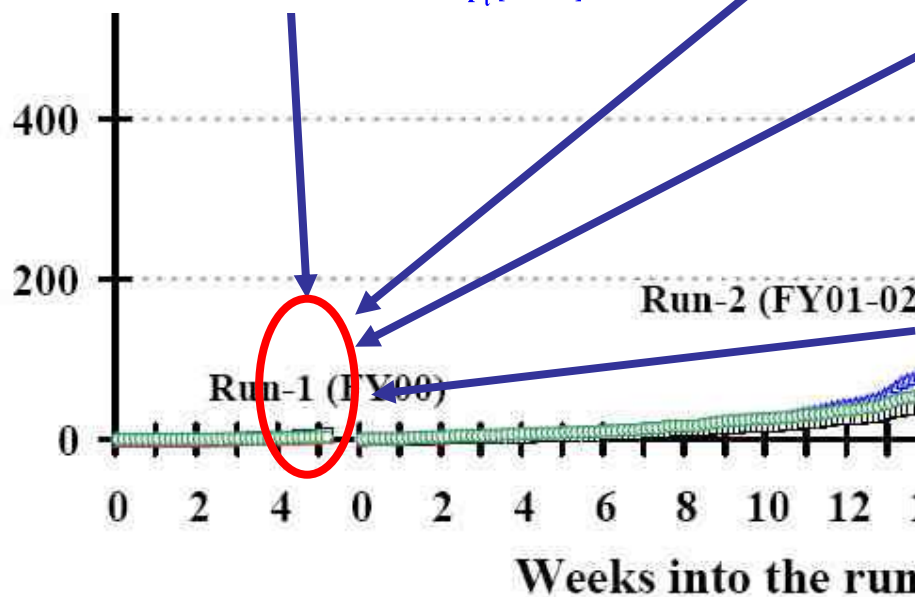
Collective Flow



Jet Quenching

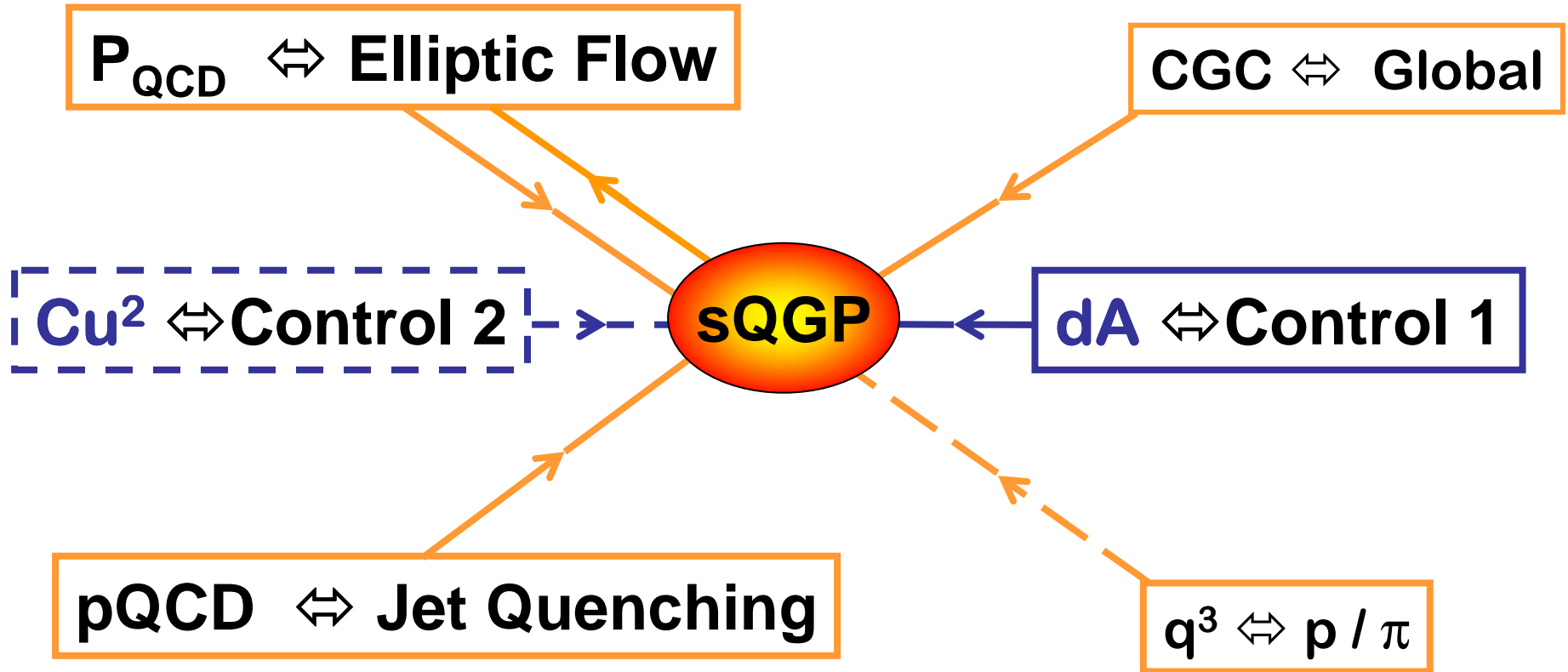


Color Glass



Empirical Evidence at RHIC that points to the Discovery of **sQGP** and CGC

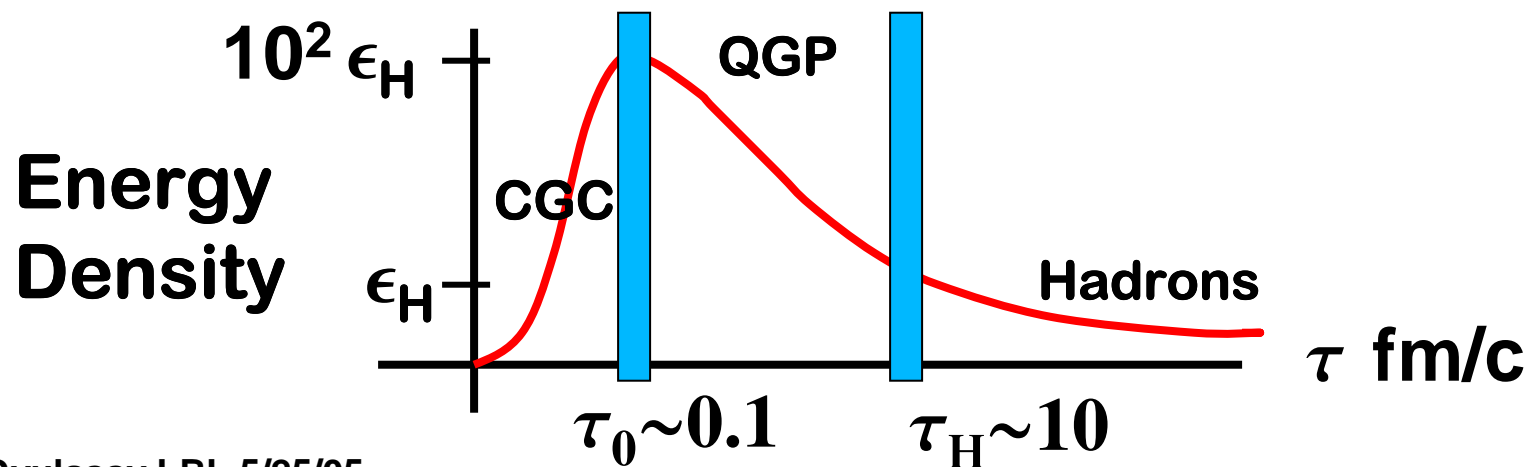
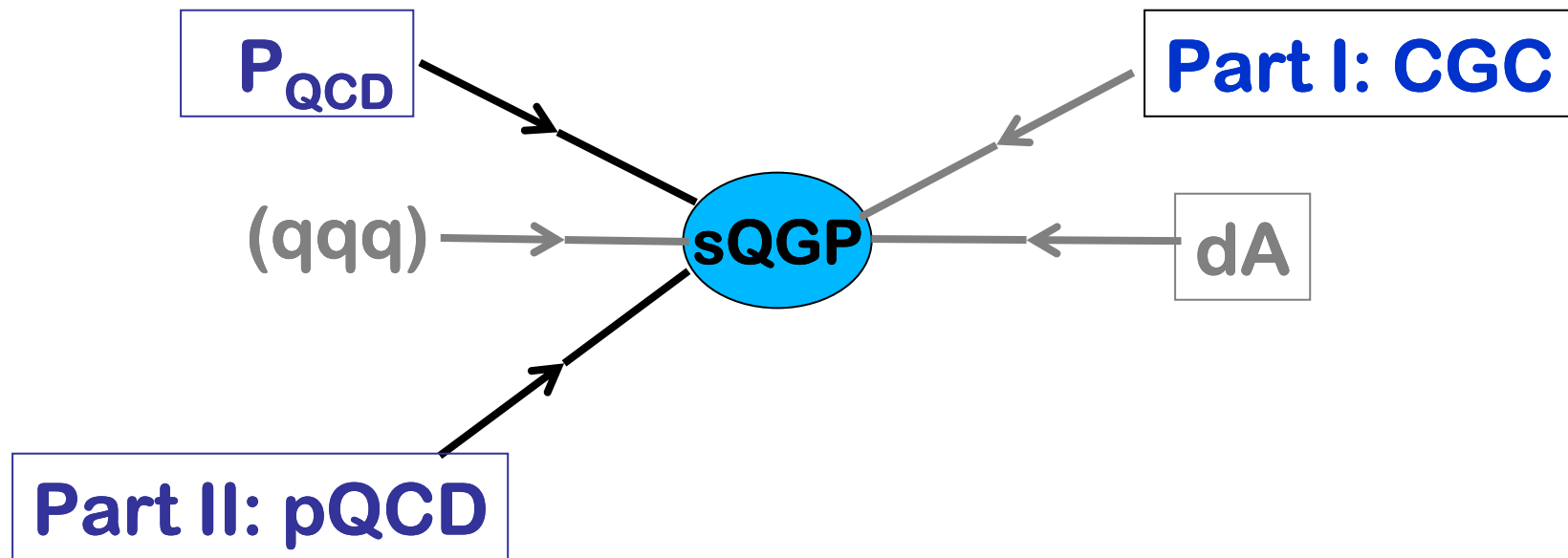
strongly coupled



$$sQGP = P_{QCD} + pQCD + dA + Q_s + q^3 + \dots$$

$$CGC = Q_s(y, A) + \dots$$

Physics of Nuclear Collisions



Importance of controlled A+A Initial Conditions

$$\partial_{\mu} T^{\mu\nu} = 0$$

Is a 1-to-1 map from Initial \rightarrow Final

sQGP must first be created !

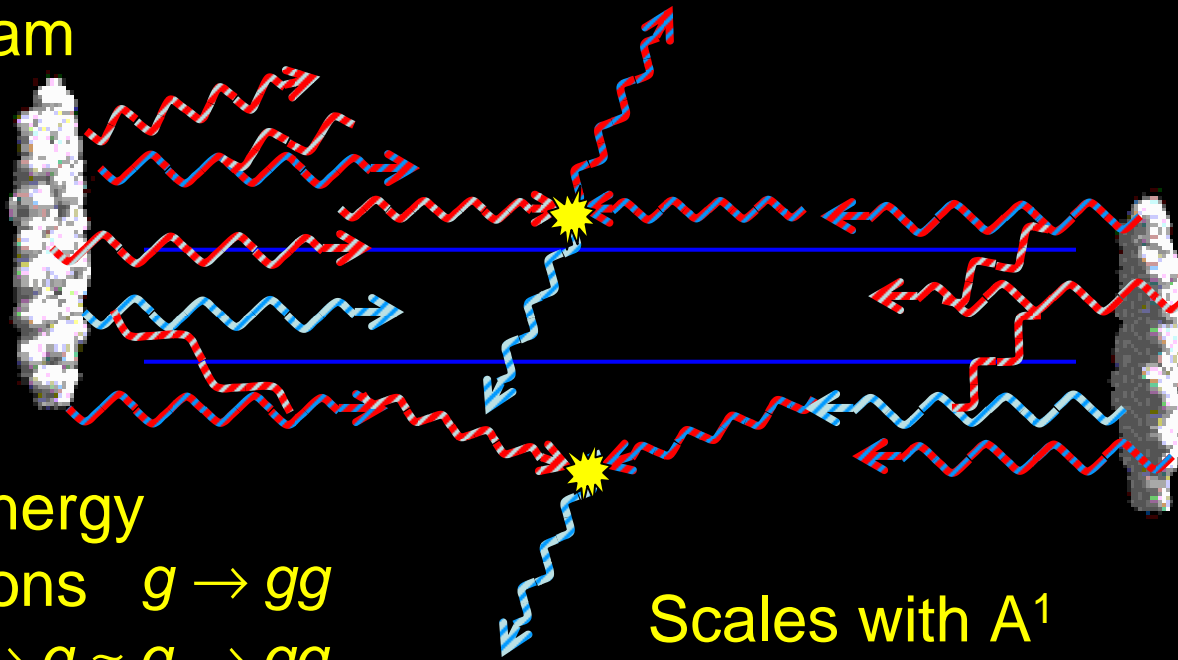
CGC is source of sQGP

sQGP Formation via CGC

High Energy Nucleus
Is equivalent to a
Weizsacker-Williams
Gluon Beam

Scales with $A^{4/3}$

$$g + g \rightarrow g + g \quad p_T > Q_s(x, A)$$



Higher Energy
More gluons $g \rightarrow gg$
Until $gg \rightarrow g \approx g \rightarrow gg$

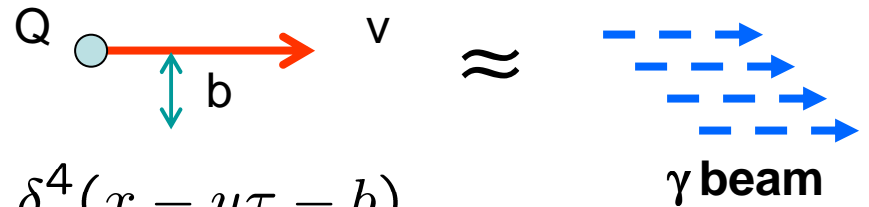
Scales with A^1

$$g' + g' \rightarrow g \quad p_T < Q_s(x, A)$$

Color Glass Condensate Saturation Scale

$$Q_s^2(x, A) \approx 2 \text{ GeV}^2 \left(\frac{10^{-2}}{x} \right)^{\frac{1}{3}} \left(\frac{A}{200} \right)^{\frac{1}{3}}$$

Equivalent Photons and Relativistic E+M



$$J^\mu(x) = Q \int d\tau c u^\mu \delta^4(x - u\tau - b)$$

$$u^\mu = \gamma(1, \vec{\beta}) \quad , \quad \underline{\beta = v/c \rightarrow 1} \quad , \quad \gamma = \frac{1}{\sqrt{1 - \beta^2}} \gg 1$$

$$\vec{E}(\vec{\rho} - \vec{b}, z - vt) = \gamma Q \frac{(\vec{\rho} - \vec{b}) - \hat{z}(z - vt)}{((\vec{\rho} - \vec{b})^2 + \gamma^2(z - vt)^2)^{3/2}}$$

$$\vec{B} = \vec{\beta} \times \vec{E} = \beta \hat{z} \times \vec{E}_\perp \quad , \quad |B|/|E| \approx 1$$

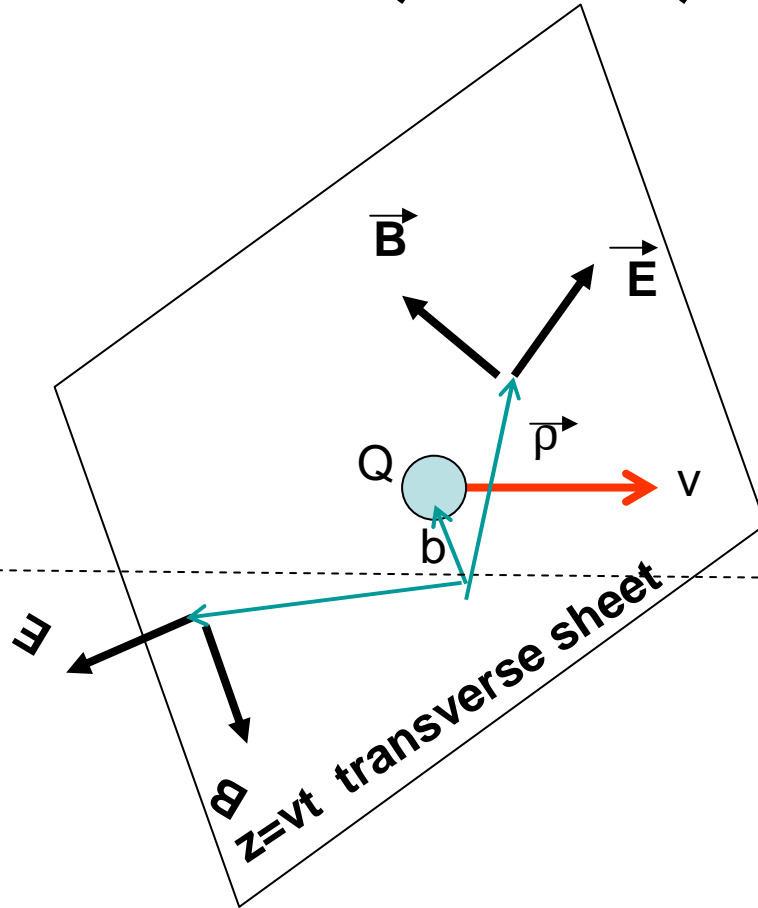
Approx transverse EM fields amplified by factor γ and squeezed within $|z - vt| \lesssim 1/\gamma$

Fermi, Weizsacker-Williams, ..., Jackson p724, Low p150

$$Q \rightarrow Q + \gamma$$

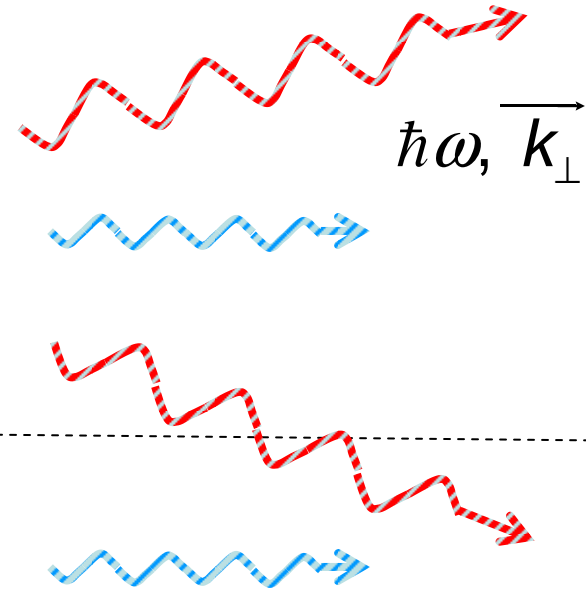
Highly Boosted Coulomb Field

= Sheet of transverse E and B



Space-Time Fields

Virtual Photons



Fourier Decomposition

$$\frac{\text{EM Energy}}{\text{unit area}} = \int_{-\infty}^{\infty} dt \frac{c}{4\pi} (\vec{E} \times \vec{B}) \cdot \hat{v} \quad \text{Poynting}$$

$$\approx \int_{-\infty}^{\infty} \frac{d\omega}{2\pi} \frac{c}{4\pi} |E_{\perp}(\vec{\rho}, \omega)|^2 \equiv \int_0^{\infty} d\omega \hbar\omega \frac{dN_{\gamma}}{d\omega d^2\vec{\rho}} \quad 4.6.12$$

Parseval ($t \Leftrightarrow \omega$)

$$\frac{dN_{\gamma}}{d\omega d^2\vec{\rho}} = \frac{c}{4\pi^2} \frac{|E_{\perp}(\vec{\rho}, \omega)|^2}{\hbar\omega} \quad 4.6.14B$$

$$\text{Total EM Energy} = \frac{c}{4\pi} \int \frac{d\omega}{2\pi} \frac{d^2\vec{k}}{(2\pi)^2} |E_{\perp}(\vec{k}, \omega)|^2 = \int d^2\vec{k} \int_0^{\infty} d\omega \hbar\omega \frac{dN_{\gamma}}{d\omega d^2\vec{k}}$$

Parseval ($\rho \Leftrightarrow \mathbf{k}$)

$$\frac{dN_{\gamma}}{d\omega d^2\vec{k}_{\perp}} = \frac{c}{(2\pi)^4} \frac{|E_{\perp}(\vec{k}_{\perp}, \omega)|^2}{\hbar\omega} \quad 4.6.14C$$

Partons Independent Only in Dilute Limit

$$A_{\perp}(\text{glue}) = \frac{dN_{\text{glue}}}{dy} \frac{c \alpha_s(Q)}{Q^2} < \pi R^2$$

Critical Packing Fraction

$$\kappa = A_{\perp}(\text{glue}) / \pi R^2 = 1$$

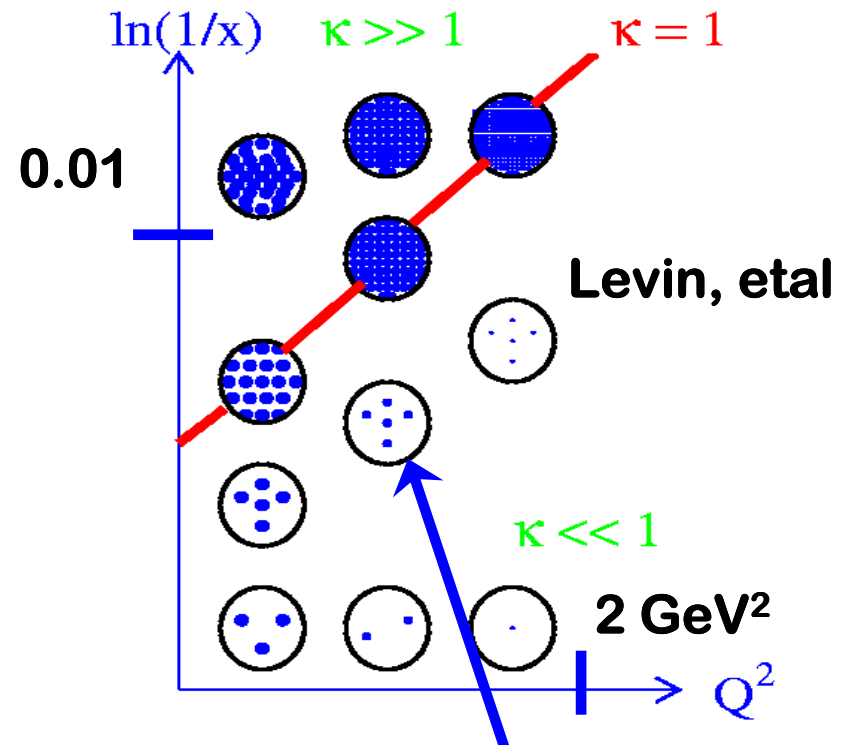
Saturation momentum scale:

$$\kappa(x, Q_s^2(x, A)) = 1$$

$$xG_A(x, Q_s^2) \propto A^{1-\delta} \left(\frac{x_0}{x}\right)^{\lambda} \text{Log } Q_s^2 \propto \frac{Q_s^2 R^2}{\alpha(Q_s)}$$

$$Q_s^2(x, A) \propto A^{0.3} x^{-0.3}$$

McLerran-Venugopalan Color Glass Condensate



Dilute Parton gas

Mueller-Qiu
Kharzeev-Levin-Nardi

“Glauber” Form Factor $T_A(k_T)$

$$\vec{E}(\vec{k}_\perp, \omega = kc, z) = \frac{e^{ikz}}{c} \vec{W}(\vec{k}_\perp, k) \left\{ \sum_a q_a e^{i\vec{k}_\perp \cdot \vec{b}_a} \right\}$$

Point charge spectral function

$$\vec{W}(\vec{k}_\perp, k) = \int d^2\vec{\rho} e^{-i\vec{k}_\perp \cdot \vec{\rho}} \left(\frac{\vec{\rho}}{\rho^2} \right) \int_{-\infty}^{\infty} \frac{du}{(u^2 + 1)^{3/2}} \exp[iu k\rho/\gamma]$$

$$\vec{W}(\vec{k}_\perp, k) = \int d^2\vec{\rho} e^{-i\vec{k}_\perp \cdot \vec{\rho}} \left(\frac{\vec{\rho}}{\rho^2} \right) \frac{2\rho k}{\gamma} K_1(k\rho/\gamma) = 4\pi i \hat{k}_\perp \frac{k}{\gamma} \int_0^\infty d\rho \rho J_1(k_\perp \rho) K_1(k\rho/\gamma)$$

$$\vec{W}(\vec{k}_\perp, k) = 4i\pi \frac{k_\perp^\vec{}}{k_\perp^2 + k^2/\gamma^2}$$

$$|\vec{W}(\vec{k}_\perp, k)|^2 = \frac{4(2\pi)^2 k_\perp^2}{(k_\perp^2 + k^2/\gamma^2)^2}$$

$$\frac{dN_\gamma}{d\omega d^2\vec{k}_\perp} = \frac{c}{(2\pi)^4} \frac{|E_\perp(\vec{k}_\perp, \omega)|^2}{\hbar\omega}$$

$$|\vec{E}(\vec{k}_\perp, \omega = kc, z)|^2 = \frac{|\vec{W}(\vec{k}_\perp, k)|^2 |T_A(\vec{k}_\perp)|^2}{c^2}$$

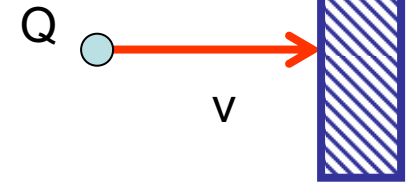
$$|\vec{W}(\vec{k}_\perp, k)|^2 = \frac{4(2\pi)^2 k_\perp^2}{(k_\perp^2 + k^2/\gamma^2)^2}$$

$$\frac{dN_\gamma}{d\omega} = \frac{2Q^2 c (2\pi)^3}{(2\pi)^4 \hbar\omega c^2} \int_0^\infty dk_\perp^2 \frac{k_\perp^2 |T_A(k_\perp)|^2}{(k_\perp^2 + \omega^2/(\gamma c)^2)^2}$$

$$|T_A(\vec{k}_\perp)|^2 = \left\langle \left| \sum_{a \in A} \frac{q_a}{Q} e^{i\vec{k}_\perp \cdot \vec{b}_a} \right|^2 \right\rangle$$

When an ultra-relativistic charge comes to a sudden stop

$$u^\mu = \gamma(1, \beta) \rightarrow (1, 0)$$



$$J^\mu(k) = Q \int_{-\infty}^{\infty} d\tau \, c u^\mu e^{\epsilon|\tau|} \exp[i(ku)\tau]$$

$$J^\mu = iQc \left(\frac{u^\mu}{(ku)} - \frac{g^{\mu 0}}{k^0} \right), \quad |J|^2 = \frac{Q^2 c^2}{k_0^2} \left(1 + \frac{1}{\gamma^2(1 - \beta\mu)^2} - \frac{2\gamma}{\gamma(1 - \beta\mu)} \right)$$

$$\frac{dI}{d^3k} = \hbar\omega \frac{dN_\gamma}{d\omega/cd^2k_\perp} = \frac{-1}{4\pi^2 c^2} |J_\mu(k)|^2$$

$$1 - \mu \approx \theta^2/2 \approx \frac{k_\perp^2}{2k^2}$$

$$\frac{dN_\gamma}{d\omega d^2k_\perp} = \frac{\alpha}{4\pi^2 k^2} \frac{1 - \mu^2}{(1 - \beta\mu)^2} \approx \frac{\alpha}{\pi^2} \frac{k_\perp^2}{(k_\perp^2 + k^2/\gamma^2)^2}$$

$$k/\gamma = xM$$

Radiation “Dead” Cone

$$\theta_{\text{cone}} = 1/\gamma = M/E$$

Exactly the same distributions of real photons as in the virtual WW field

The cloud is “shaken off” by sudden ac(de)celeration

What is a CGC?

Unitarity limit of Virtual Gluon Cloud

$$\text{Rate}(gg \rightarrow g) \approx \text{Rate}(g \rightarrow gg)$$

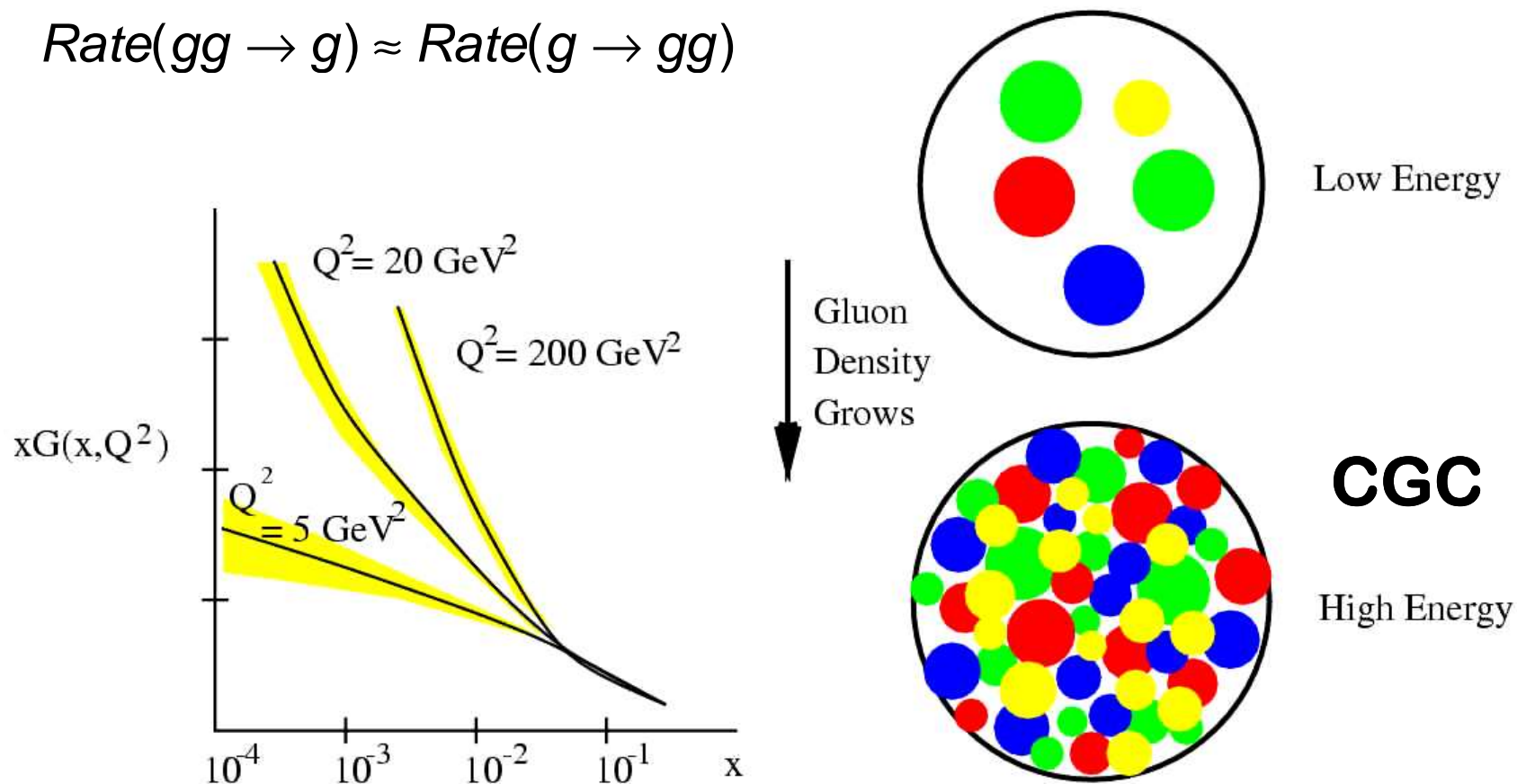


Figure 3: (a) The HERA data for the gluon distribution function as a function of x for various values of Q^2 . (b) A physical picture of the low x gluon density inside a hadron as a function of energy

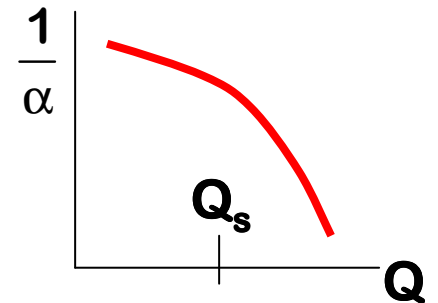
Gribov, Levin, McLerran, Venugopalan, Mueller...

Unintegrated Gluon phase space density

$$xG(x, Q^2) \propto \alpha \text{Log } Q^2 < c \frac{Q^2 R^2}{\alpha(Q)}$$

$$\frac{dn(x, k^2)}{dy d^2r dk^2} = \frac{1}{\pi R^2} \frac{dxG(x, k^2)}{dk^2} \sim \begin{cases} \propto \frac{1}{\alpha} & \text{if } Q^2 < Q_s^2 \\ \propto \frac{\alpha}{k^2 R^2} & \text{if } Q^2 > Q_s^2 \end{cases}$$

Phase space saturation

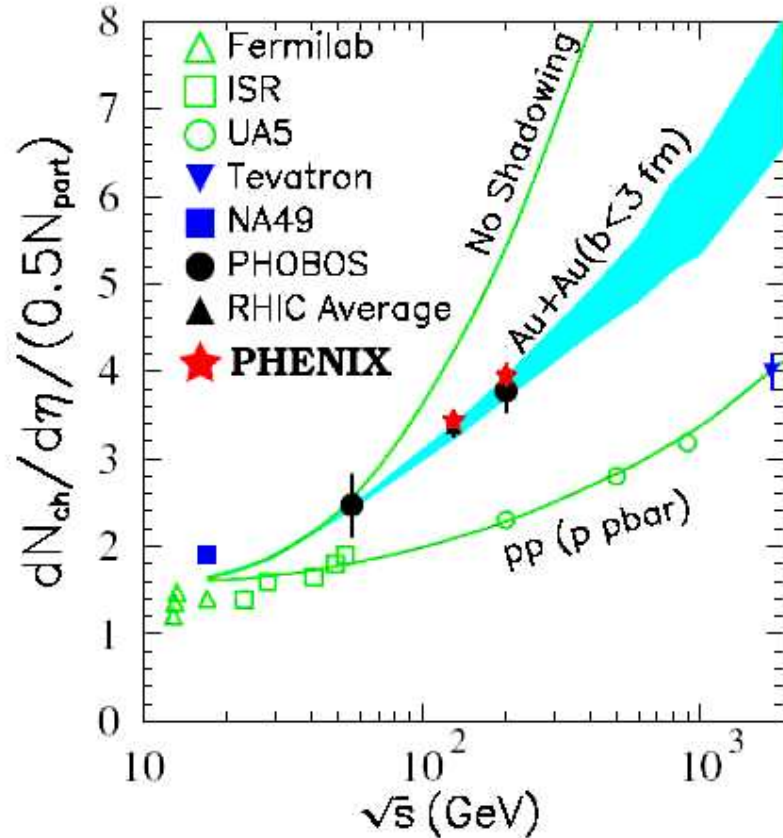


$$\frac{dN}{dy} \propto xG(x, Q_s^2) \propto \frac{Q_s^2 R^2}{\alpha(Q_s)} \propto s^{\lambda/2} A \text{Log } A$$

Predicts Slow growth Of multiplicity

Global Evidence for saturating CGC initial state at RHIC

$$Q_s^2(x, A) \approx 2 \text{ GeV}^2 \left(\frac{10^{-2} A}{x \cdot 200} \right)^{0.3}$$



Gluon Saturation below $k_T < Q_s$

Limits Rapid Growth of pQCD mini-jets

Corresponds to Deep Gluon Shadowing in $x < 0.01$ region

$$N_{ch} = \rho_s(Q_s) A + \rho_H(Q_s) A^{4/3}$$

RHIC data prove Q_s varies with s and A

Nuclear Glue Structure RHIC vs LHC

RHIC is a sQGP machine with a partial view of CGC

CGC at RHIC

$$\frac{dN_g}{dy} \approx c \frac{Q_s^2 R^2}{\alpha_s(Q_s^2)} \left(1 - \frac{2Q_s}{\sqrt{s}} e^{|y|} \right)^4 \quad \text{Kinematically Limited at } y = 3$$

$$Q_s^2(x, A) \approx 2 \text{ GeV}^2 \left(\frac{10^{-2}}{x} \frac{A}{200} \right)^{0.3}$$

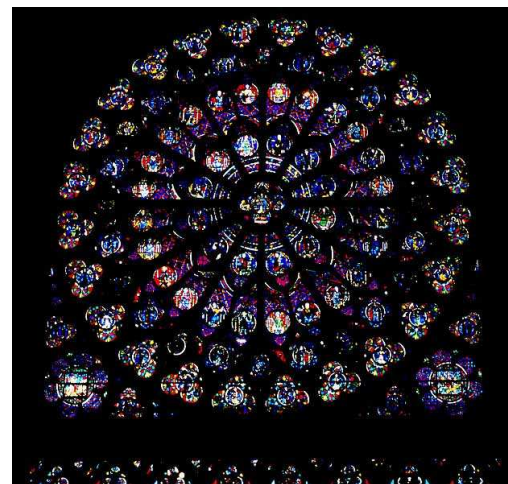
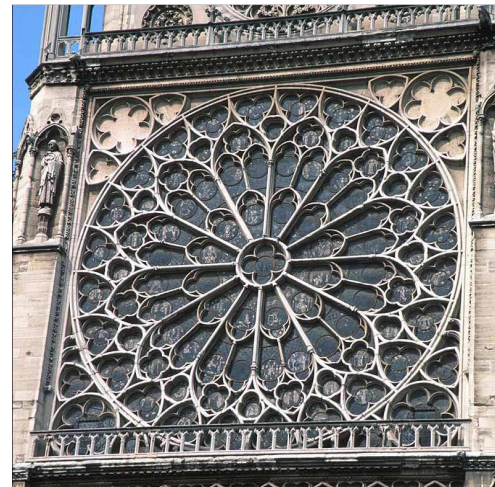
$$\left. \begin{array}{l} \xrightarrow[y=3 \text{ } p_T=2]{\text{RHIC}} \rightarrow 5 \text{ GeV}^2 \\ \xrightarrow[y=0 \text{ } p_T=2]{\text{LHC}} \rightarrow 5 \text{ GeV}^2 \\ \xrightarrow[y=3 \text{ } p_T=2]{\text{LHC}} \rightarrow 14 \text{ GeV}^2 \end{array} \right\}$$

$$\frac{dN_g}{dy} \approx c \frac{Q_s^2 R^2}{\alpha_s(Q_s^2)}$$

Kinematics Free at $y \leq 3$

CGC at LHC

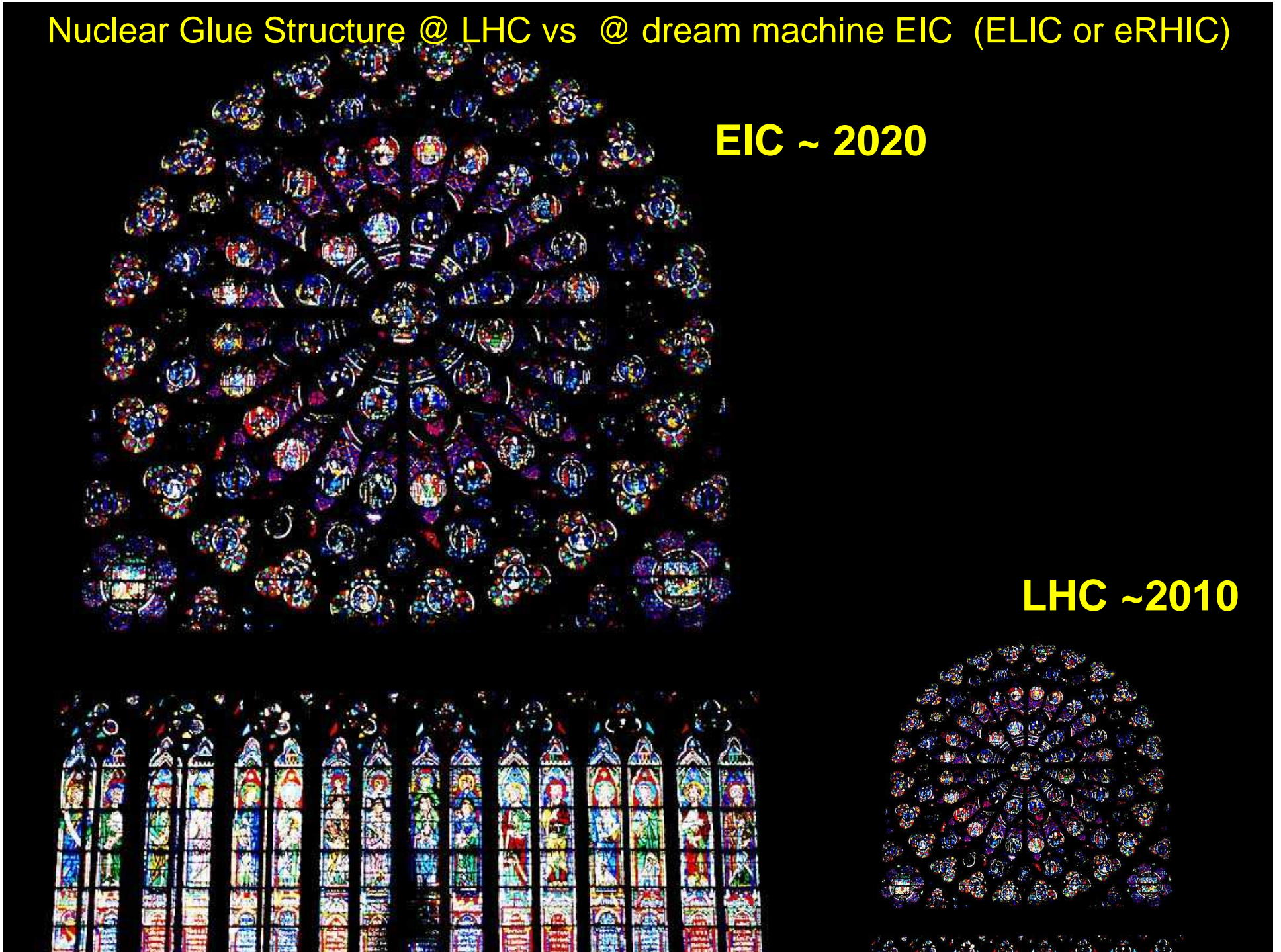
LHC is a CGC machine with a partial view of sQGP

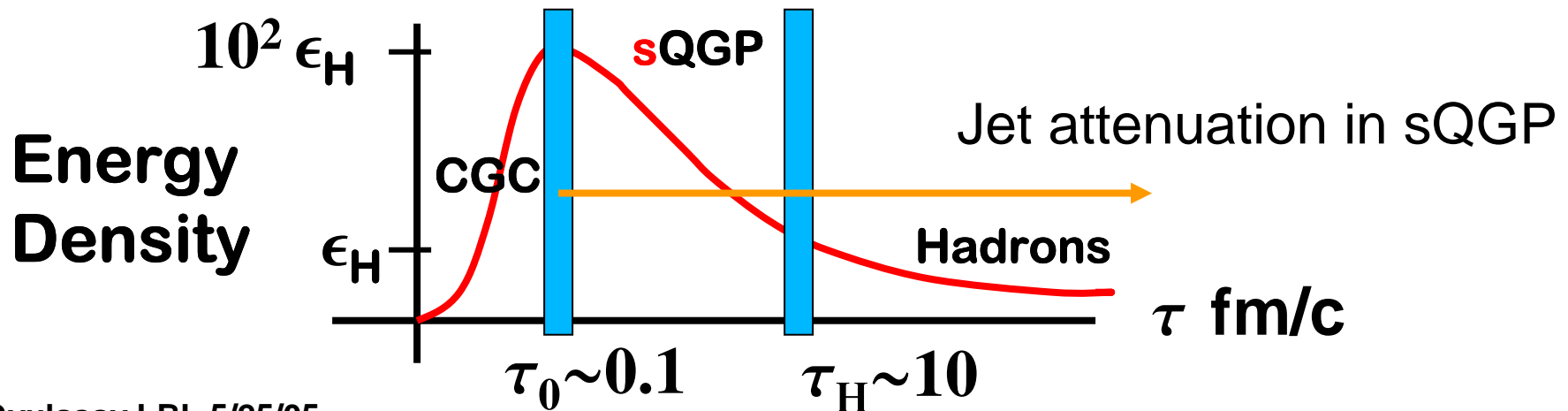
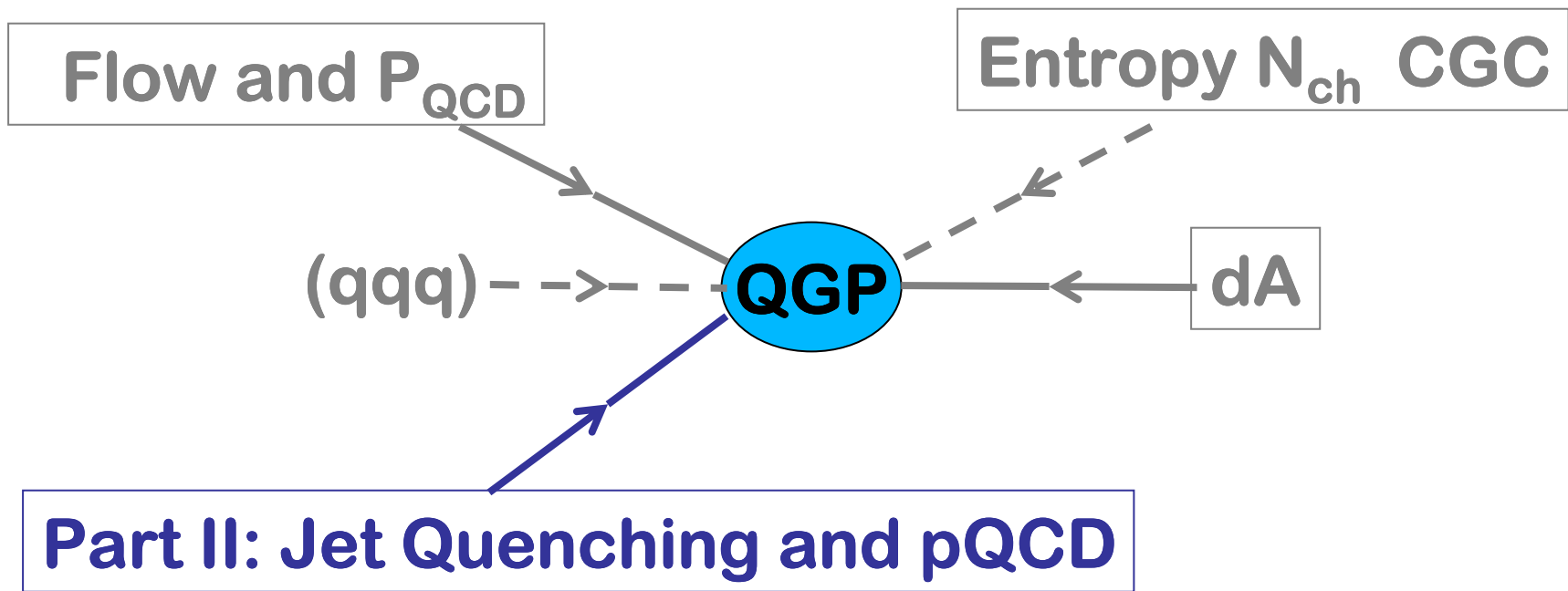


Nuclear Glue Structure @ LHC vs @ dream machine EIC (ELIC or eRHIC)

EIC ~ 2020

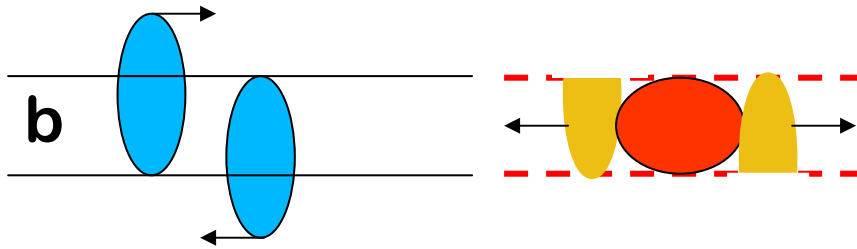
LHC ~2010





Geometric Scaling of High p_T Observables :

Centrality Selected Single Inclusive $\left(\frac{dN^{AB \rightarrow h+X}}{dy_h d^2p_{\perp,h}} \right)_{N_{part}, \sqrt{s}}$



Participating nucleons

$$N_{part}(b) = 2 \int d^2s T_A(s + \frac{b}{2}) (1 - e^{-\sigma T_A(s - \frac{b}{2})})$$

Rare processes scale with

$$N_{coll}(b) = \sigma_{in} T_{AB}(b) \sim \{N_{part}(b)\}^{4/3}$$

$$T_{AB}(b) = \int d^2s T_A(b-s) T_B(s) \approx \frac{A^{4/3}}{40 \text{ mb}}$$

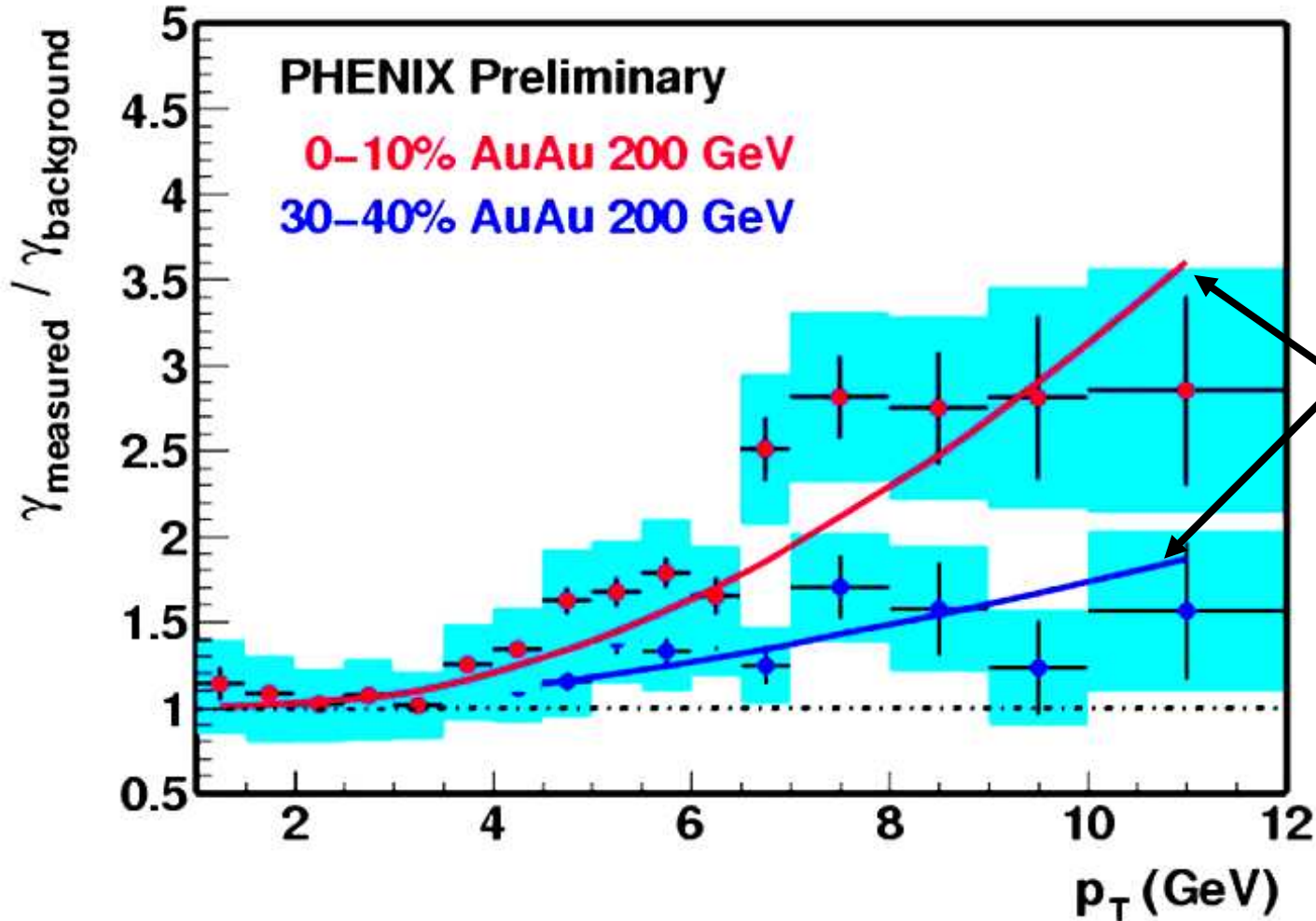
Binary collision density

Nuclear Modifications Factor

$$R_{AB}(p_{\perp} | y, h, N_{part}, \sqrt{s}) = \frac{dN^{AB \rightarrow h}}{T_{AB} d\sigma^{pp-h}} = \frac{1}{N_{coll}} \frac{dN^{AB \rightarrow h}}{dN^{pp-h}}$$

N_{coll} scaling observed for direct photons

$$N_{\gamma}(\text{Au} + \text{Au}, p_T > 6) \approx N_{\text{coll}} \times N_{\gamma}(\text{p} + \text{p}, p_T > 6)$$



$$N_{\text{coll}} \times dN^{\text{pp} \rightarrow \gamma}$$

Vogelsang NLO

N_{coll} scaling of charm production

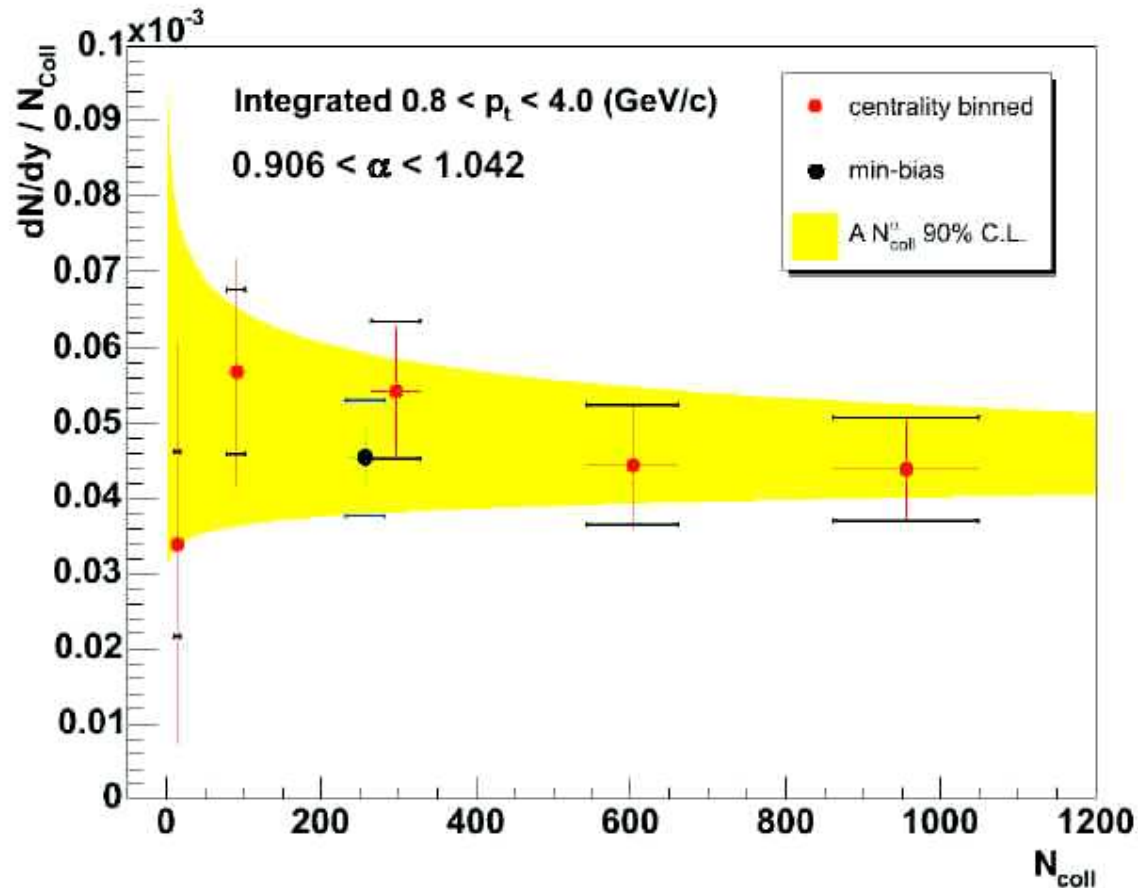
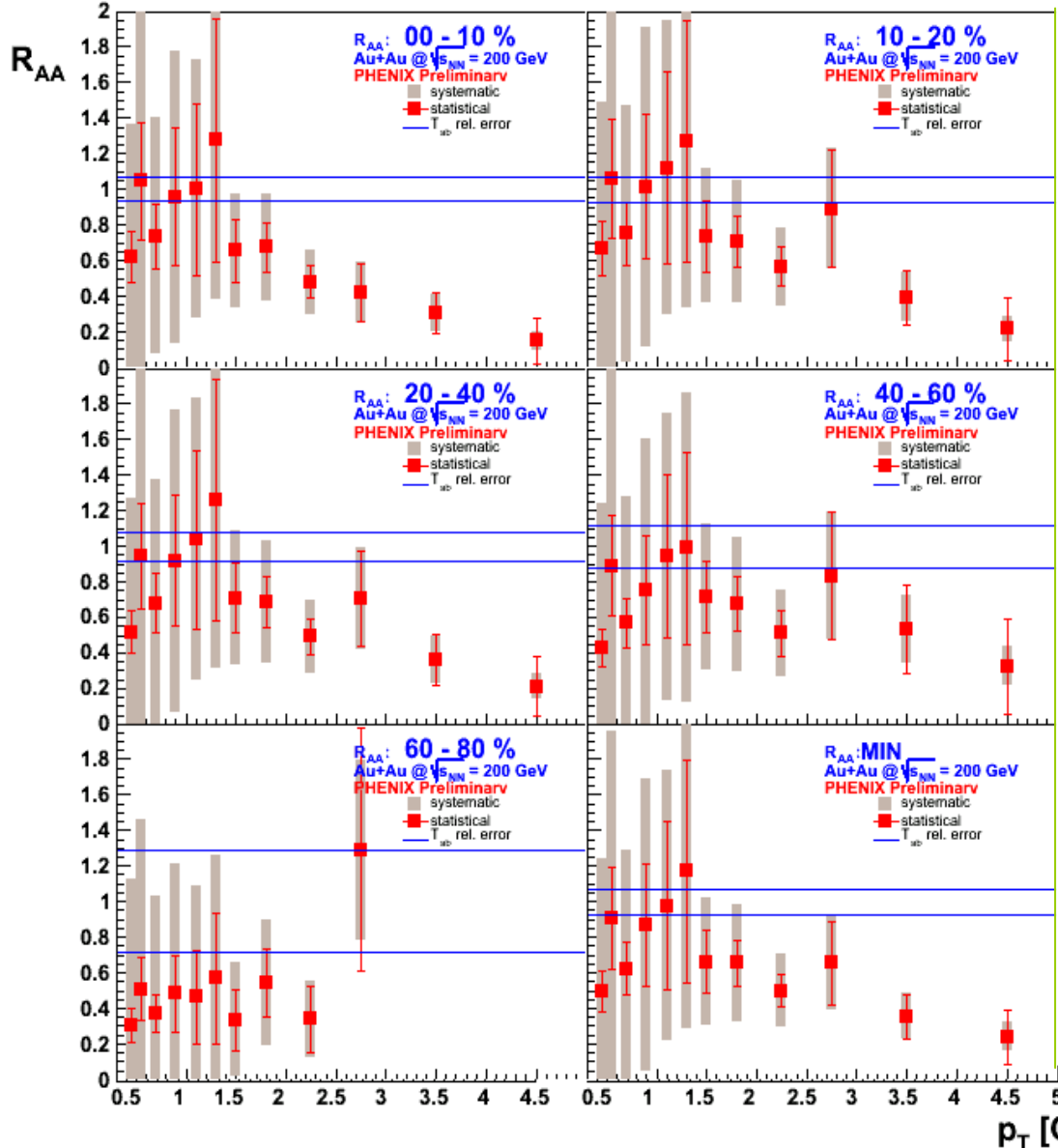


FIG. 34: Non-photonic electron yield ($0.8 < p_T < 4.0$ GeV/c), dominated by semi-leptonic charm decays, measured in Au+Au collisions at $\sqrt{s_{NN}} = 200$ GeV scaled by N_{coll} as a function of N_{coll} .

Weird and Puzzling *Preliminary* Charm Suppression Data



First Au+Au $\rightarrow e$ X data showed
no hint of heavy quark energy
loss ! ??

PHENIX Collaboration
(K. Adcox *et al.*)

Phys.Rev.Lett.88:192303,2002

$R_{AA}(p_T)$ for non-photonic
single electrons in Au+Au

**!Significant reduction at
high p_T suggest sizable
energy loss!**

Sergey Butsyk

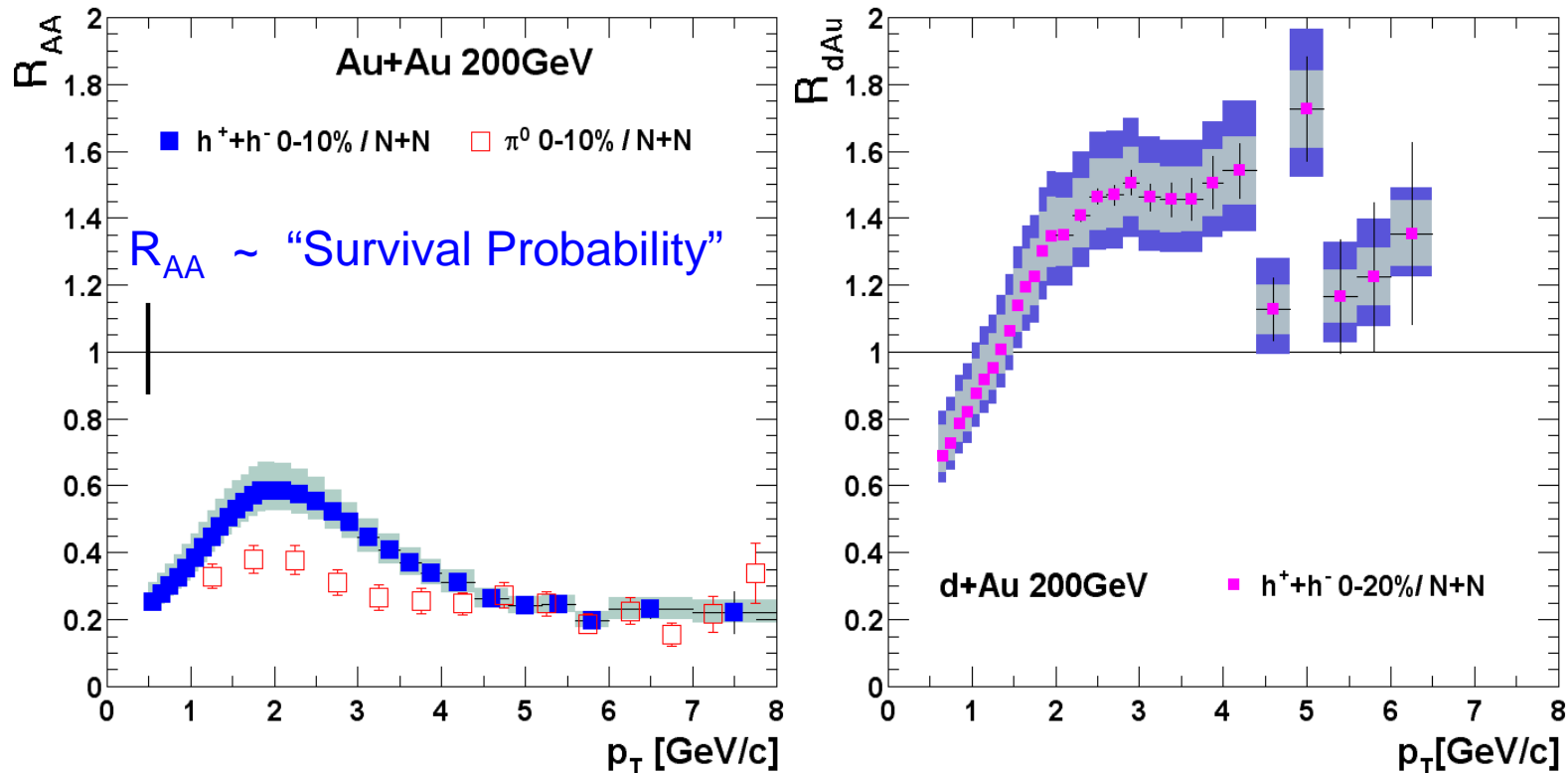
(21st Winter Workshop on Nuclear
Dynamics)

THE primary advantage of RHIC is its proven ability to perform

Dedicated Control **p+p** and **p+A** as well as **B+A** experiments as well as \sqrt{s}

Required to sort the competing novel physics of sQGP from its CGC source

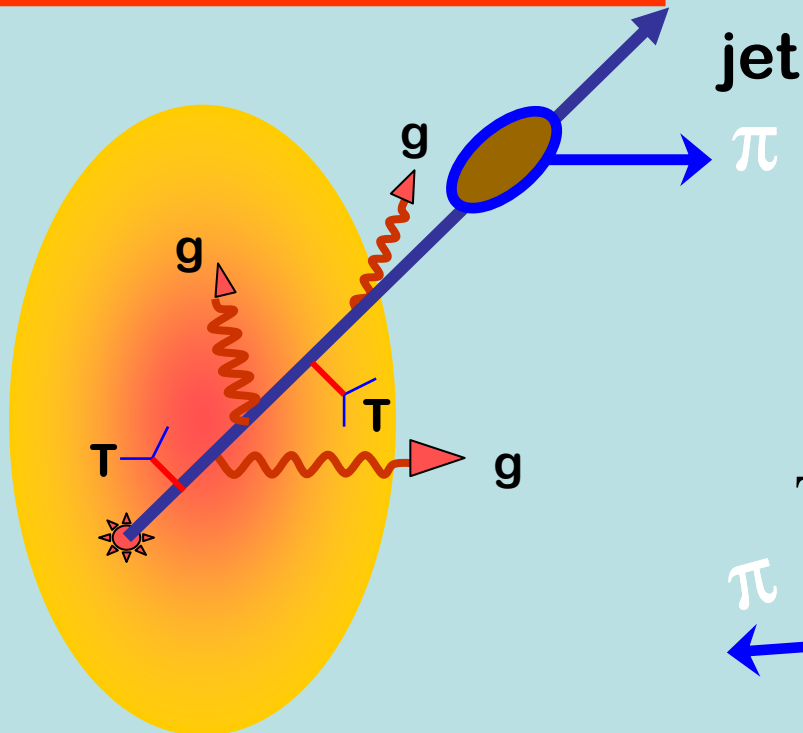
Nuclear Modification Factor $R_{BA}(p_{\perp}) = dN^{BA \rightarrow \pi} / T_{BA}(b) d\sigma^{pp \rightarrow \pi}$



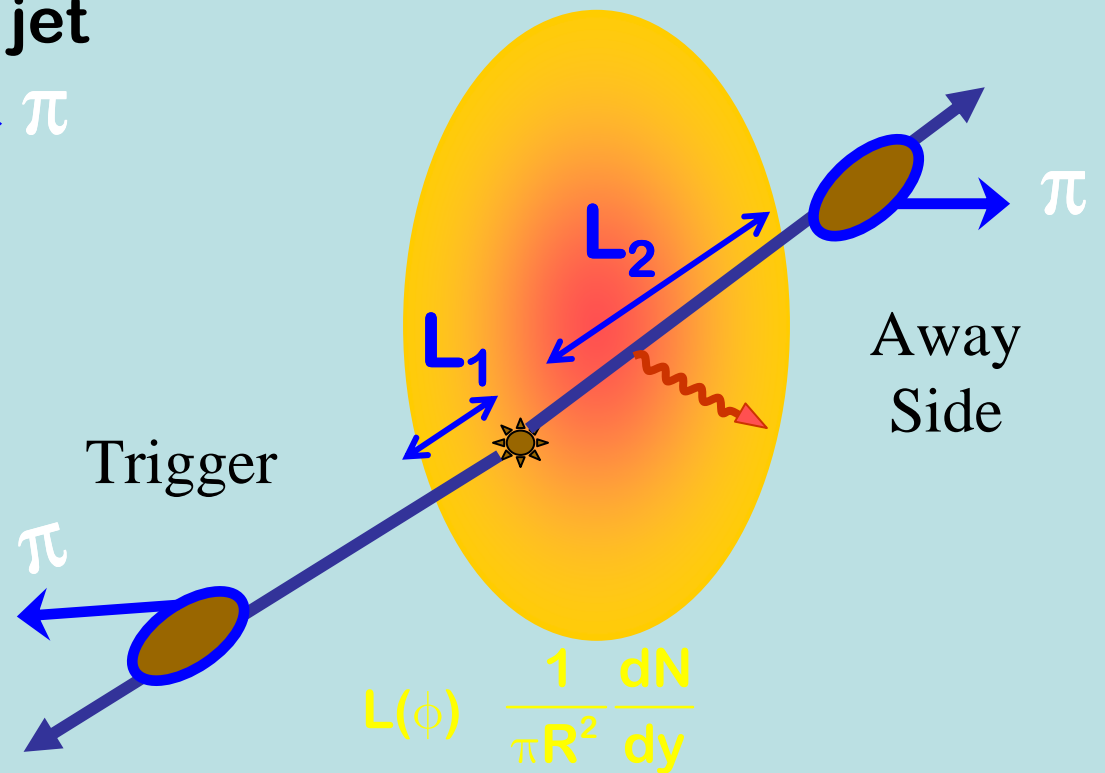
High p_T Tomography of the sQGP

M.G., P. Levai, I.Vitev ; X.N. Wang, E.Wang, B.W.Zhang
Review nucl-th/0302077

Single Hadron Tomography



Di-Hadron Tomography



$$L(\phi) \frac{1}{\pi R^2} \frac{dN}{dy}$$

$$\Delta E_{GLV} \sim C_{Jet} C_T \alpha_S^3 \ln \frac{p_T}{\mu^2 L} \int d\tau \tau \rho(\tau, r(\tau))$$

**Final Result to Arbitrary Order in Opacity $(L/\lambda)^n$
for M_Q and $m_g > 0$ (DG, Nucl.Phys.A 733, 265 (04))**

$$x \frac{dN^{(n)}}{dx d^2\mathbf{k}} = \frac{C_R \alpha_s}{\pi^2} \frac{1}{n!} \int \prod_{i=1}^n \left(d^2\mathbf{q}_i \frac{L}{\lambda_g(i)} [\bar{v}_i^2(\mathbf{q}_i) - \delta^2(\mathbf{q}_i)] \right) \times$$

$$\times \left(-2 \tilde{C}_{(1,\dots,n)} \cdot \sum_{m=1}^n \tilde{B}_{(m+1,\dots,n)(m,\dots,n)} \left[\cos \left(\sum_{k=2}^m \Omega_{(k,\dots,n)} \Delta z_k \right) - \cos \left(\sum_{k=1}^m \Omega_{(k,\dots,n)} \Delta z_k \right) \right] \right)$$

Hard, Gunion-Bertsch, and Cascade ampl. in GLV generalized to finite M

$$\tilde{H} = \frac{\mathbf{k}}{\mathbf{k}^2 + m_g^2 + M^2 x^2}, \quad \tilde{C}_{(i_1 i_2 \dots i_m)} = \frac{(\mathbf{k} - \mathbf{q}_{i_1} - \mathbf{q}_{i_2} - \dots - \mathbf{q}_{i_m})}{(\mathbf{k} - \mathbf{q}_{i_1} - \mathbf{q}_{i_2} - \dots - \mathbf{q}_{i_m})^2 + m_g^2 + M^2 x^2}$$

$$\tilde{B}_i = \tilde{H} - \tilde{C}_i, \quad \tilde{B}_{(i_1 i_2 \dots i_m)(j_1 j_2 \dots j_n)} = \tilde{C}_{(i_1 i_2 \dots j_m)} - \tilde{C}_{(j_1 j_2 \dots j_n)}$$

$$\omega_{(m,\dots,n)} = \frac{(\mathbf{k} - \mathbf{q}_m - \dots - \mathbf{q}_n)^2}{2xE} \rightarrow \Omega_{(m,\dots,n)} \equiv \omega_{(m,\dots,n)} + \frac{m_g^2 + M^2 x^2}{2xE}$$

Generalizes GLV $M_Q = m_g = 0$ (NPB594(01))

Leading order in opacity

(M. Djordjevic, MG)

$$\frac{dE_{ind}^{(1)}}{dx} = \frac{C_R \alpha_S}{\pi} \frac{L}{\lambda} E \int \frac{d\mathbf{k}^2}{\mathbf{k}^2 + m_g^2 + M^2 x^2} \int \frac{d^2 \mathbf{q}_1}{\pi} \frac{\mu^2}{(\mathbf{q}_1^2 + \mu^2)^2} \times$$
$$\times 2 \frac{\mathbf{k} \cdot \mathbf{q}_1 (\mathbf{k} - \mathbf{q}_1)^2 + (m_g^2 + M^2 x^2) \mathbf{q}_1 \cdot (\mathbf{q}_1 - \mathbf{k})}{\left(\frac{4Ex}{L}\right)^2 + ((\mathbf{k} - \mathbf{q}_1)^2 + M^2 x^2 + m_g^2)^2},$$

LPM effects are
smaller for **heavy** than
for light quarks!

“Dead-cone” effect is more
subtle than for the 0th order
energy loss

Initial Jet distribution $\rho_g(\mathbf{p}) = \frac{dN_g}{dyd^2p} \sim \frac{c}{p^{n-7}}$

No medium Pion distribution $\rho_\pi(\mathbf{p}_\pi) = \int_{p_\pi}^{\infty} \frac{dp}{p_\pi} \rho_g(\mathbf{p}) D_{\pi/g}(z = \frac{p_\pi}{p})$

In medium $\mathbf{p} \rightarrow \mathbf{p} - \Delta\mathbf{p}(\mathbf{p}) \approx \mathbf{p}(1-\epsilon)$

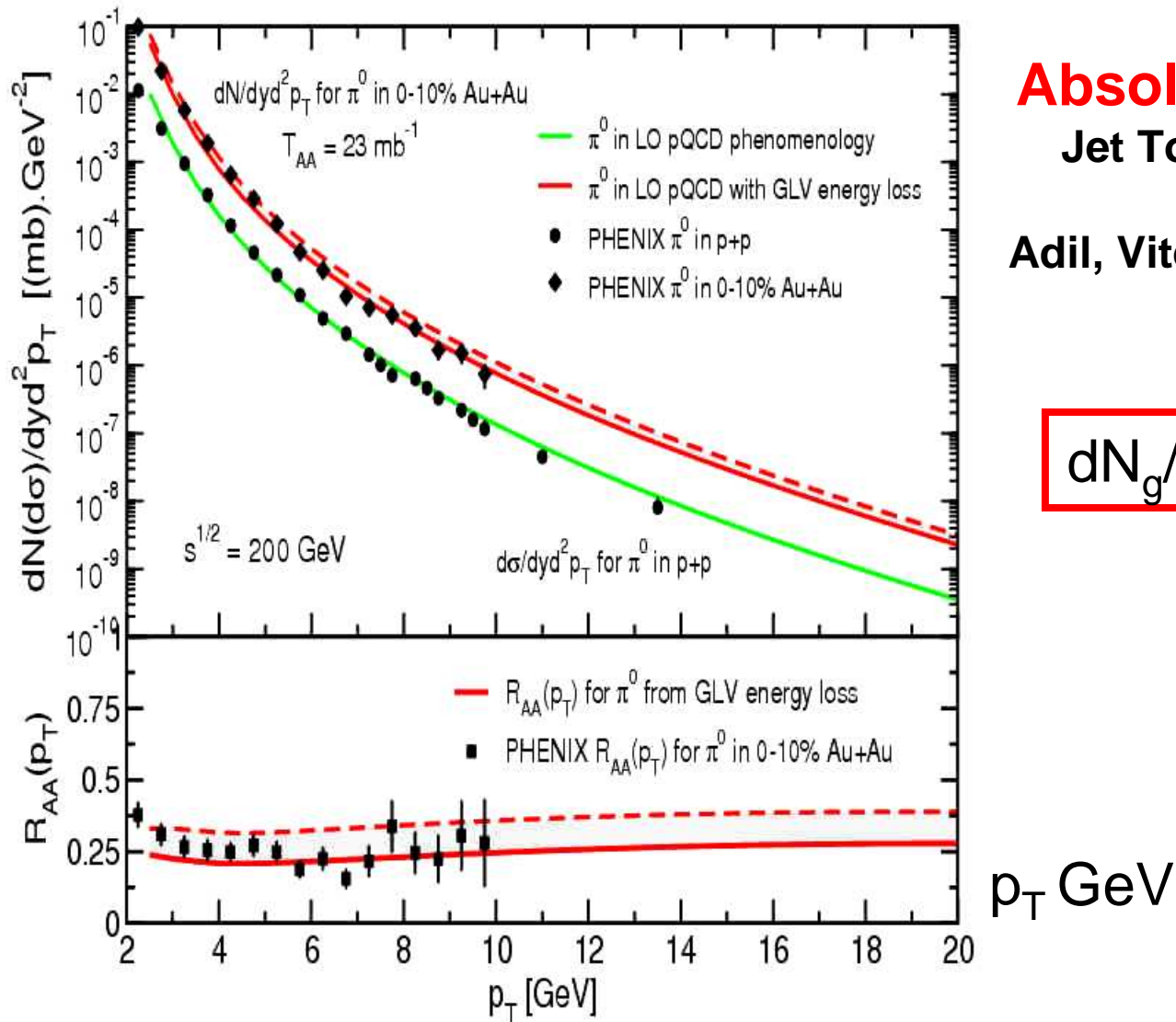
$D(z) \rightarrow D'(z) = \frac{\theta(1-\epsilon-z)}{1-\epsilon} D(z' = \frac{z}{1-\epsilon})$

Quenched Pions $\rho_\pi(\mathbf{p}_\pi, \epsilon) = \int_{\frac{p_\pi}{(1-\epsilon)}}^{\infty} \frac{dp}{p_\pi} \rho_g(\mathbf{p}) \frac{1}{(1-\epsilon)} D_{\pi/g}(z' = \frac{p_\pi}{p(1-\epsilon)})$

For $\rho_g(\mathbf{p}) \propto 1/p^n$: $\rho_\pi^{\text{quenched}}(\mathbf{p}_\pi) = \langle (1-\epsilon)^{n-2} \rangle \rho_g(\mathbf{p}_\pi)$

Quench Factor $R_{AA} = \frac{\langle \rho_\pi(\mathbf{p}, \epsilon) \rangle}{\rho_\pi(\mathbf{p}, 0)} = \langle (1-\epsilon)^{n-2} \rangle = (1-Z\langle \epsilon \rangle)^{n-2}$

Fluctuations reduce ΔE by factor $Z \sim 0.5$



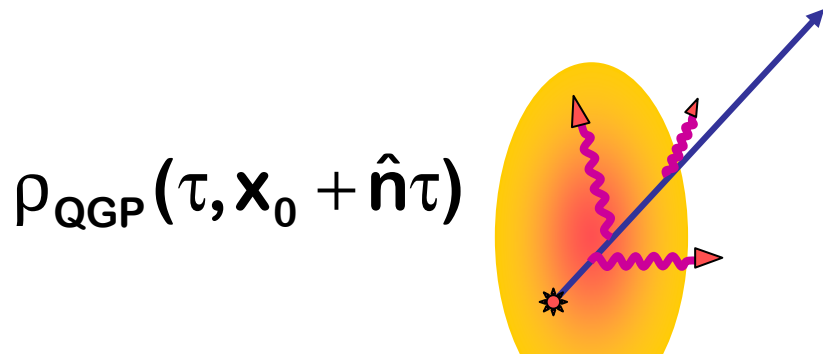
Absolute Scale Jet Tomography

Adil, Vitev, MG (2005)

$$dN_g/dy=900-1200$$

$$dN_{AB \rightarrow \pi} = T_{AB} \otimes \left(f_{a/A} \otimes f_{b/B} \right)_{\Delta k_T}^{\text{shad}} \otimes d\sigma_{ab \rightarrow c} \otimes P(\Delta E) \otimes D_{\pi/c}$$

Azimuthal $v_2(p_t)$ Tomography



STAR

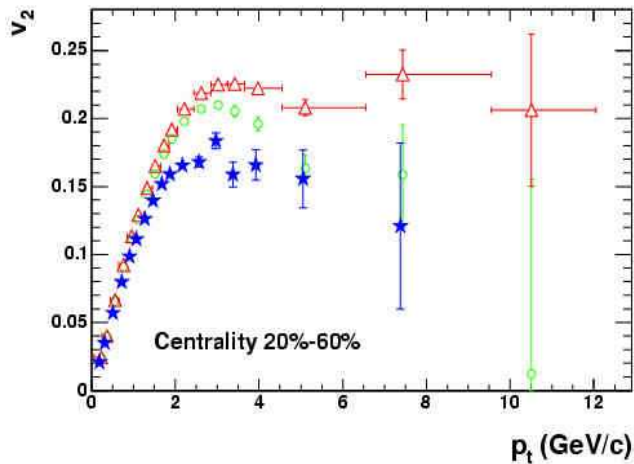
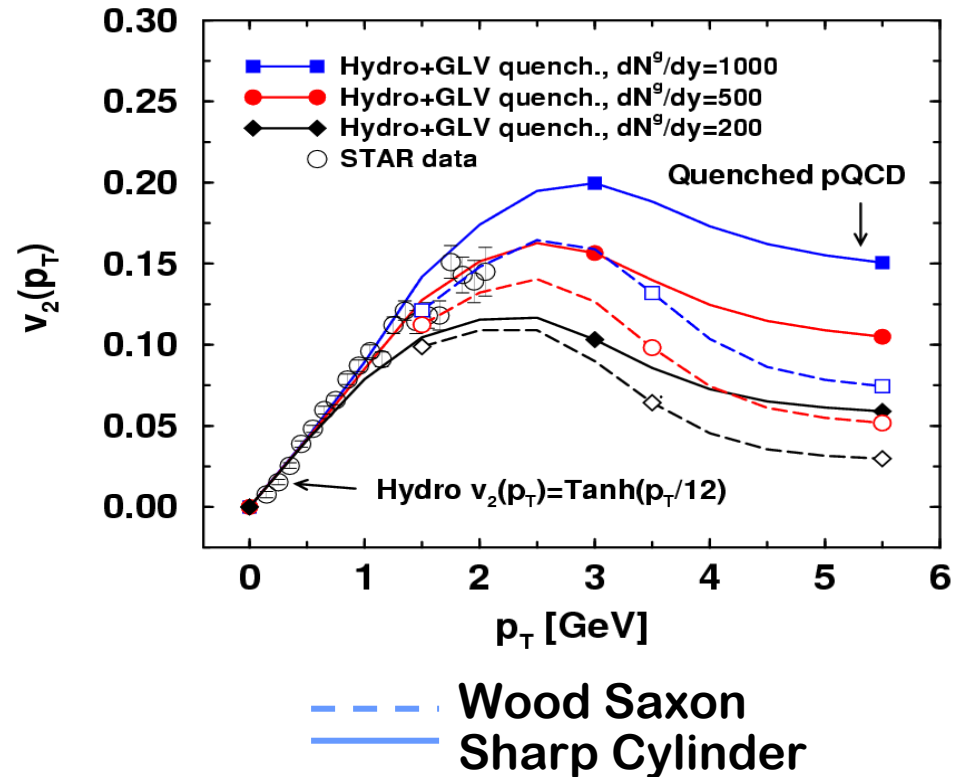


FIG. 2: (color online) v_2 of charged particles as a function of transverse momentum from the two-particle cumulant method (triangles) and four-particle cumulant method (stars). See text for explanation of the open circles. Only statistical errors are shown.

I. Vitev, X.N. Wang, MG, PRL86(01)



High $v_2(10 \text{ GeV})$ Still Open Problem

Four independent calibrations of Initial **QGP** density

$$\epsilon(\tau_0) \approx 100 \epsilon_0 = 15 \text{ GeV/fm}^3$$

1. Bjorken Backward extrapolation

$$\begin{aligned} E_T / N_\pi &= 0.5 \text{ GeV}, \quad dN_\pi / dy = 1000, \\ \tau_0 &= 1/p_0 = 0.2 \text{ fm}/c, \quad V = (0.2 \text{ fm})\pi R^2 = 30 \text{ fm}^3 \\ \epsilon_{\text{Bj}} &= 500 \text{ GeV} / 30 \text{ fm}^3 = 100 \epsilon_0 \end{aligned}$$

2. Hydrodynamic initial condition needed for $v_2(p_T)$

$$\epsilon_{\text{Hydro}} > 2 \epsilon_{\text{Bj}} = 500 \text{ GeV} / 30 \text{ fm}^3 = 100 \epsilon_0$$

KHH
TS
HN

3. Jet Tomography: $dN_g/dy = 1000$

$$\epsilon_{\text{Jets}} \approx \epsilon_{\text{Bj}} \approx 100 \epsilon_0$$

GLV
WW

4. Gluon saturation $p_T < Q_s$ predicted

$$dN_g/dy = 1000 \text{ at } Q_{\text{sat}} = 1 \text{ GeV at } y=0$$

MB
McV
EKRT